



LAKE2K

Version 1.05

**A Modeling Framework for Simulating Lake Water Quality
(BETA TEST VERSION)**

Draft User's Manual and Documentation



Walden Pond at Concord, MA

Steve Chapra, James Martin & Kyle Flynn
November 15, 2023

Chapra, S.C., Martin, J.L., and Flynn, K.F. 2023. LAKE2K: A Modeling Framework for Simulating Lake Water Quality (Version 1.05): Documentation and User's Manual. Civil and Environmental Engineering Dept., Tufts University, Medford, MA., Steven.Chapra@tufts.edu

CONTENTS

1	INTRODUCTION.....	5
2	GETTING STARTED.....	7
3	USERS MANUAL.....	11
3.1	OVERVIEW.....	11
3.2	MODEL PARAMETER WORKSHEETS.....	12
3.2.1	LAKE2K Worksheet.....	12
3.2.2	Elevation-Area Worksheet.....	13
3.2.3	Inflow Data Worksheet.....	13
3.2.4	Outflow Worksheet.....	14
3.2.5	Initial Conditions Worksheet.....	15
3.2.6	Vertical Mixing Worksheet.....	15
3.2.7	Meteorology Worksheet.....	16
3.2.8	Ice Worksheet.....	17
3.2.9	Light and Heat Worksheet.....	17
3.2.10	Rates Worksheet.....	18
3.3	DATA WORKSHEETS.....	20
3.3.1	Physical Data Worksheet.....	21
3.3.2	Water Quality Data Worksheets.....	21
3.3.3	Miscellaneous Data Worksheet.....	21
3.4	Output Worksheets.....	22
3.5	Output Charts.....	24
3.6	Navigating the Sheets and Charts.....	25
4	PHYSICS.....	28
4.1	Water Balance.....	28
4.1.1	Inflow.....	29
4.1.2	Precipitation.....	29
4.1.3	Evaporation.....	29
4.1.4	Outflow.....	29
4.2	Vertical Segmentation and Mixing.....	30
5	TEMPERATURE MODEL.....	33
5.1	Surface Heat Flux.....	33
5.1.1	Solar Radiation.....	34
5.1.2	Atmospheric Long-wave Radiation.....	35
5.1.3	Water Long-wave Radiation.....	36
5.1.4	Conduction and Convection.....	36

5.1.5	Evaporation and Condensation.....	37
5.2	Ice Model.....	37
6	CONSTITUENT MODEL	41
6.1	Constituents and General Mass Balance	41
6.2	Reaction Fundamentals	42
6.2.1	Biochemical Reactions	42
6.2.2	Stoichiometry of Organic Matter.....	43
6.2.3	Temperature Effects on Reactions.....	44
6.3	Constituent Reactions.....	44
6.3.1	Specific Conductance (s).....	45
6.3.2	Phytoplankton (a_p).....	45
6.3.3	Herbivorous zooplankton (z_h).....	48
6.3.4	Carnivorous zooplankton (z_c)	49
6.3.5	Particulate Organic Carbon (c_p).....	50
6.3.6	Dissolved Organic Carbon (c_d).....	50
6.3.7	Organic Nitrogen (n_o).....	51
6.3.8	Ammonia Nitrogen (n_a).....	51
6.3.9	Nitrate Nitrogen (n_n).....	52
6.3.10	Organic Phosphorus (p_o).....	52
6.3.11	Inorganic Phosphorus (p_i).....	53
6.3.12	Inorganic Suspended Solids (m_i)	53
6.3.13	Dissolved Oxygen (o).....	53
6.4	LIGHT MODEL AND SECCHI DEPTH	55
6.5	SOD/Nutrient Flux Model.....	56
6.5.1	Diagenesis.....	57
6.5.2	Ammonium.....	59
6.5.3	Nitrate.....	60
6.5.4	Methane.....	61
6.5.5	SOD.....	62
6.5.6	Inorganic Phosphorus	63
6.5.7	Solution Scheme.....	64
6.5.8	Supplementary Fluxes	65
7	APPENDIX A: DENSITY OF WATER.....	67
8	APPENDIX B: O'CONNOR'S GAS TRANSFER MODEL	69
9	REFERENCES	71

Part I

User's Manual

This section provides a description of how to apply the model.

1 INTRODUCTION

LAKE2K (L2K) is a model designed to compute seasonal trends of water quality in one-dimensionally (1D) vertically stratified lakes. L2K is implemented within the Microsoft Windows environment. It is programmed in the Windows macro language Visual Basic for Applications (VBA). Excel is used as the graphical user interface.

This documentation and user's manual has been written for the beta version of the model. The model has already been alpha tested; that is, it has been debugged and subjected to numerical tests to confirm that it yields numerically accurate results. A beta version represents software that is intended to be run by selected users prior to general distribution.

2 GETTING STARTED

Installation is required for many water-quality models. This is not the case for LAKE2K because the model is packaged as an Excel Workbook. The program is written in Excel's macro language: Visual Basic for Applications or VBA. The Excel Workbook's worksheets and charts are used to enter data and display results. Consequently, you merely have to open the Workbook to begin modeling. The following are recommended step-by-step instructions on how to obtain your first model run.

Step 1: Create a folder named LAKE2K to hold the workbook and its data files. For example, in the following example, a folder named LAKE2K is created on the C:\ drive. Create a subdirectory of LAKE2K called DataFiles.

Step 2: Copy the L2KMaster file (L2KMaster0105.xlsm) to C:\LAKE2K.

Step 3: Open Excel and make sure that your macro security level is set to medium. This can be done using the menu commands: Tools → Macro → Security. Make certain that the Medium radio button is selected as shown in Figure 1.

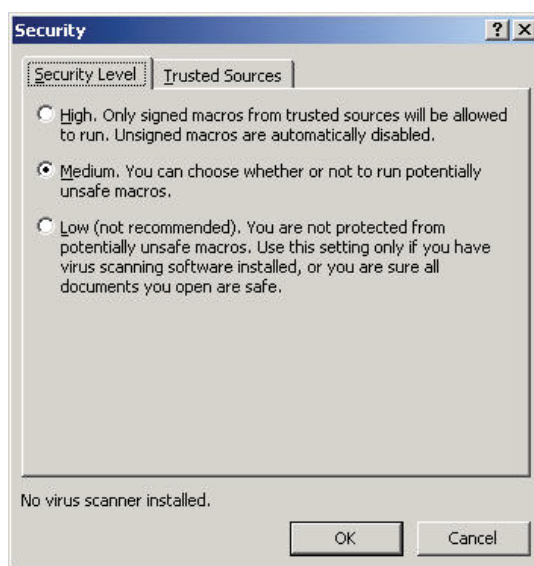
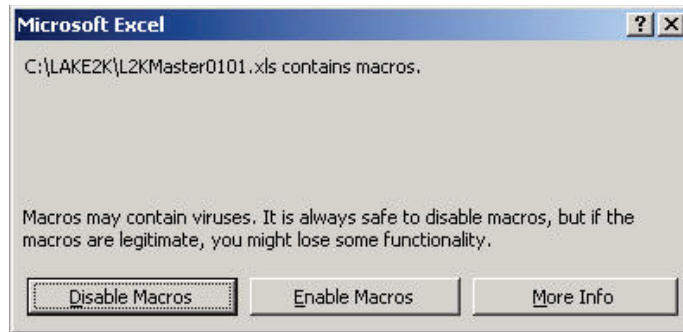



Figure 1 The Excel Macro Security Level dialogue box. In order to run L2K, the Medium level of security should be selected.

Step 4: Open L2KMaster0105.xlsm. When you do this, the Macro Security Dialogue Box will be displayed (Figure 2). Alternatively, on newer PCs, you may find that Microsoft has blocked macros from the source because the file is untrusted.



 **SECURITY RISK** Microsoft has blocked macros from running because the source of this file is untrusted. [Learn More](#)

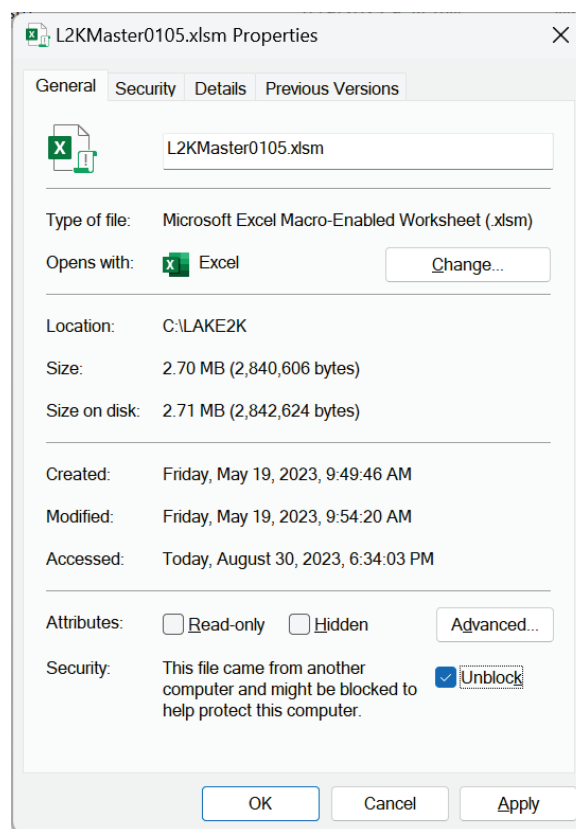


Figure 2 The Excel Macro security dialogue box. To run L2K, the Enable Macros button must be selected as indicated in the top panel. Alternatively, if macros are blocked in newer Excel versions, you will need to modify the L2KMaster0105.xlsm file properties as shown in the bottom panel

Click on the Enable Macros button. Or for newer PCs, provide file permissions to open the workbook. To do this, browse to the folder where the L2KMaster0105.xlsm file is located and right click on the file and then open Properties (Alt+Enter). Then make sure the Unblock button is checked on the General tab (Figure 2).

Step 5: Immediately save the file as L2K0105.xlsm. This will be the Excel Workbook that you will use on a routine basis. If for some reason, you modify L2K0105.xlsm in a way that makes it unusable, you can always go back to L2KMaster0105.xlsm as a backup.

Step 6: On the LAKE2K worksheet, go to cell B10 and enter the path to the file directory where L2K0105.xlsm is located: C:\LAKE2K\DataFiles as shown in Figure 3.


B10		C:\LAKE2K\DataFiles				
	A	B	C	D	E	F
1	LAKE2K				RUN	
2	Lake Water Quality Model					
3	Steve Chapra					
4						
5					Open Old File	
6						
7	System ID:					
8	River name	Lake Nalms				
9	File name	NALMSLake				
10	Directory where file saved	C:\LAKE2K\DataFiles				
11	Latitude	40.000	degrees			
12	Elevation	1600.0	meters			
13	Calculation:					
14	Calculation step	0.50000	day			
15	Print step	2.00000	day			
16	Initial time	1/1/93				
17	Final time	12/31/94				
18	Time of last calculation	0.35	minutes			

Figure 3 The LAKE2K worksheet showing the entry of the file path into cell B10.

Step 7: Click on the Run button. LAKE2K will begin to execute. You can follow the progress of the execution on the status bar that is shown in the bottom left corner of the worksheet (Figure 4).

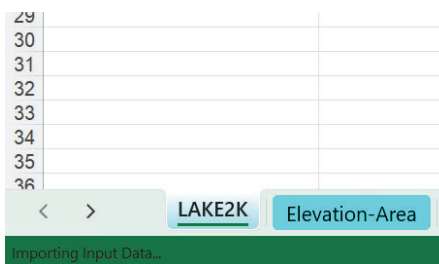


Figure 4 The LAKE2K Status Bar is positioned at the lower left corner of the worksheet. It allows you to follow the progress of a model run.

If the program runs properly, the temperature plot will be displayed at the end of the run. If it does not work properly, two possibilities exist:

First, you may be using an old version of Microsoft Office. Although Excel is downwardly compatible for some earlier versions, L2K will not work with very old versions.

Second, you may have made a mistake in implementing the preceding steps. A common mistake is to have mistyped the file path that you entered in cell B10. If this is the case, you will receive an error message (Figure 5).

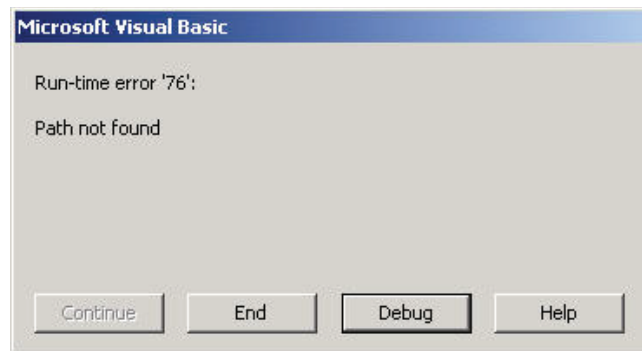


Figure 5 An error message that will occur if you type the incorrect file path into cell B10 on the LAKE2K worksheet.

If this occurs, click on the end button. This will terminate the run and bring you back to the Excel Workbook. You should then move back to the LAKE2K worksheet and correct the file path entry on the LAKE2K worksheet. Note that the same error will occur if you did not set up your directories with the correct names as was specified above.

Step 8: On the LAKE2K worksheet click on the Open Old File button. Browse to get to the directory: C:\LAKE2K\DataFiles. You should see that a new file has been created with the name specified in cell B9 and the extension .l2k. Click on the Cancel button to return to L2K.

Note that every time that L2K is run, a data file will be created with the file name specified in cell B9 on the LAKE2K worksheet (Figure 3). The program automatically affixes the extension .l2k to the file name and stores the file in the directory specified in cell B10. Since this will overwrite the file, make certain to change the file name when you perform a new application.

3 USERS MANUAL

3.1 OVERVIEW

The computer code used to implement the calculations for LAKE2K is written in Visual Basic for Applications (VBA). Excel serves as the user interface. A series of worksheets is used to enter model parameters and lake data. Model results and data are displayed on worksheets and as a series of Excel charts.

Color is used to signify whether information is to be input by the user or output by the program:

- **Pale Blue** designates variable and parameter values that are to be entered by the user.
- **Pale Yellow** designates data that the user enters. The data are then displayed on graphs generated by L2K. Hence, such data is optional.
- **Pale Green** designates output values generated by L2K.
- **Pale Pink** is graphical output of computations generated by L2K.
- **Dark solid colors** are used for labels and should not be changed.

All worksheets include two buttons (Figure 6):

- **Open Old File.** When this button is clicked, the file browser will automatically open to allow you to access a data file that was previously generated by L2K. All LAKE2K data files have the extension, *.l2k.
- **Run.** This button causes L2K to execute and to create a data file that holds the input values. The data file can then be accessed later using the **Open Old File** button.

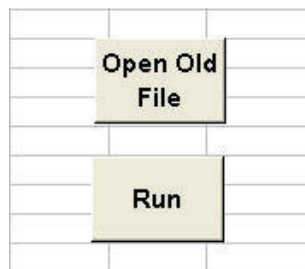


Figure 6. The buttons used in L2K.

The following sections describe the worksheets that comprise the L2K interface.

3.2 MODEL PARAMETER WORKSHEETS

A series of worksheets are used to enter information required to run the model. In current versions of Microsoft Office, these worksheets are distinguished by turquoise tabs.

3.2.1 LAKE2K Worksheet

The LAKE2K Worksheet (Figure 7) is used to enter general information regarding a particular model application.

	A	B	C	D	E
1	LAKE2K				
2	Lake Water Quality Model				RUN
3	Steve Chapra				
4					
5					Open Old File
6					
7	System ID:				
8	Lake name	Lake Nalms			
9	File name	NALMSLake			
10	Directory where file saved	C:\LAKE2K\DataFiles			
11	Latitude	40.000	degrees		
12	Elevation	1600.0	meters		
13	Calculation:				
14	Calculation step	0.50000	day		
15	Print step	5.00000	day		
16	Initial time	1/1/93			
17	Final time	12/31/94			
18	Time of last calculation	0.16	minutes		

Figure 7. The LAKE2K worksheet.

Lake name. Name of the lake being modeled. After the program is run, this name along with the date, is displayed on all sheets and charts.

File name. This is the name of the data file generated when L2K is run.

Directory where file saved. This specifies the complete path to the directory where the data file is saved.

Latitude. The user must enter the lake's latitude in decimal degrees.

Elevation. The user must enter the lake's surface elevation above sea level in meters.

Calculation step. This is the time step used for the calculation. It must be less than or equal to a day. If the user enters a value greater than 1 day, the program automatically sets the calculation step to 1 day.

Print step. This is the time step for which results are displayed. It must be greater than or equal to the calculation step. If the user enters a value less than the calculation step, the program automatically sets the print step to 1 day.

Initial time. This is the start time of the calculation entered as a data using the format MM/DD/YR.

Final time. This is the end time of the calculation entered as a data using the format MM/DD/YR.

Time of last calculation (output). The computer automatically displays the computer time required for the simulation.

3.2.2 Elevation-Area Worksheet

This worksheet (Figure 8) is used to enter the lake's hypsographic information in the form of an elevation-area curve. This information is entered from the deepest part of the lake to the highest possible surface elevation. When the program is executed, the volume below each elevation is computed and displayed in column C. A plot of the area and volume versus elevation is also displayed.

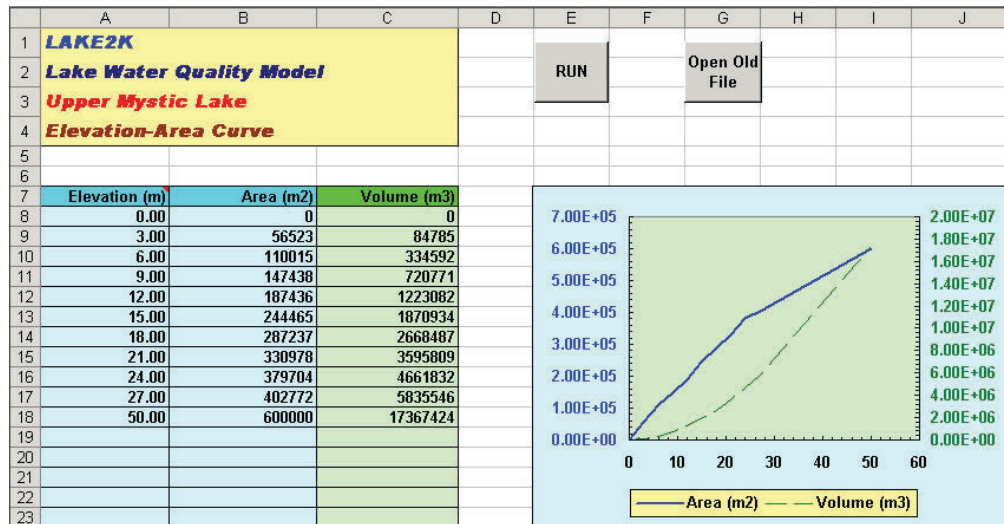


Figure 8. The Elevation-Area worksheet that is used to enter the lake's hypsographic data.

3.2.3 Inflow Data Worksheet

This worksheet is used to enter time series of the inflow data as series of dates and values. The lake's inflow is entered in columns A and B whereas the time series of inflow temperature and concentrations are entered in the remaining columns (Figure 9). The program uses linear interpolation to determine intermediate values. Note that each time series must encompass the simulation time series as specified in cells B16 and B17 of the LAKE2K worksheet.

	A	B	C	D	E	F	G	H
1	LAKE2K							
2	Lake Water Quality Model				RUN	Open Old File		
3	Lake Name							
4	Inflow Data							
5								
6	Flow		Temperature		Conductivity		Inorganic Suspended Solids	
7	t (d)	Qin (m³/s)	t (d)	Temp (°C)	t (d)	Cond (umhos)	t (d)	ISS (mg/L)
8	1/1/93	0.93	1/1/93	0.50	1/1/93	300.00	1/1/93	2.0
9	1/8/93	0.95	1/8/93	0.50	12/31/97	300.00	12/31/97	2.0
10	1/23/93	0.881	1/23/93	2.40				
11	2/7/93	0.805	2/7/93	1.90				
12	2/22/93	0.762	2/22/93	1.50				
13	3/9/93	0.719	3/9/93	4.80				
14	3/24/93	0.938	3/24/93	7.80				
15	4/8/93	0.327	4/8/93	7.20				
16	4/23/93	0.974	4/23/93	11.10				
17	5/8/93	0.376	5/8/93	13.30				
18	5/23/93	3.261	5/23/93	16.20				

Figure 9. The Inflow Data worksheet.

3.2.4 Outflow Worksheet

This worksheet is used to enter information required to compute the lake's outflow (Figure 10).

	A	B	C	D	E
1	LAKE2K				
2	Lake Water Quality Model				
3	Lake Washington				
4	Outflow				
5					
6	Outflow Mode	Time Series (epi)			
7					
8	Time series of outflows			Stage-Discharge	
9	t (d)	Qout (m3/s)		Elev (m)	Qout (m3/s)
10	1/1/00	39.637			
11	12/31/01	39.637			
12					
13					
14					
15					
16					

Figure 10. The Outflow worksheet.

Seven approaches can be used to compute outflow. The desired method is chosen using the pull-down menu in cell B6.

1. **Flowout(epi)=Flowin.** The outflow is set equal to the inflow, and none of the other inputs on the Outflow worksheet are used. For this case, the outflow exits the lake from the epilimnion. Note that if the Outflow Mode is left blank, this is the default option.
2. **Flowout(meta)=Flowin.** The outflow is set equal to the inflow, and none of the other inputs on the Outflow worksheet are used. For this case, the outflow exits the lake from the metalimnion.
3. **Flowout(hypo)=Flowin.** The outflow is set equal to the inflow, and none of the other inputs on the Outflow worksheet are used. For this case, the outflow exits the lake from the hypolimnion.
4. **Time Series (epi).** The user can enter a time series of outflows into columns A and B. The program uses linear interpolation to determine values between the entered dates. For this case, the outflow exits the lake from the epilimnion.
5. **Time Series (meta).** The user can enter a time series of outflows into columns A and B. The program uses linear interpolation to determine values between the entered dates. For this case, the outflow exits the lake from the metalimnion.
6. **Time Series (hypo).** The user can enter a time series of outflows into columns A and B. The program uses linear interpolation to determine values between the entered dates. For this case, the outflow exits the lake from the hypolimnion.

7. **Stage-Discharge.** The user can enter a stage-discharge curve in tabular form in columns D and E. The program uses linear interpolation to determine intermediate.

Note that if any of the time series options are chosen (4 through 6) the series must encompass the simulation time series as specified in cells B16 and B17 of the LAKE2K worksheet.

3.2.5 Initial Conditions Worksheet

This worksheet is used to enter initial conditions for lake elevation and the model state variables. As in Figure 11, values are entered for epilimnion, metalimnion and hypolimnion. The elevation corresponds to the depth of the top of each layer as measured upwards from the lake's bottom (by definition, the lake bottom equals an elevation of zero).

	A	B	C	D	E
1	LAKE2K				
2	Lake Water Quality Model				
3	Lake Washington				
4	Initial Conditions				
5					
6					
7	Variable	Epilimnion	Metalimnion	Hypolimnion	Units
8	Elevation of top of layer	64.000	54.000	50.000	m
9	Temperature	8.000	8.000	8.000	C
10	Specific conductance	400.000	400.000	400.000	umhos
11	ISS	1.000	1.000	1.000	mgD/L
12	POC	0.100	0.100	0.100	mgC/L
13	DOC	0.500	0.500	0.500	mgC/L
14	Norg	150.000	150.000	150.000	µgN/L
15	NH4	20.000	20.000	20.000	µgN/L
16	NO3	200.000	200.000	200.000	µgN/L
17	Porg	10.000	10.000	10.000	µgP/L
18	Pinorg	10.000	10.000	10.000	µgP/L
19	Siorg	0.000	0.000	0.000	µgSi/L
20	Siinorg	1500.000	1500.000	1500.000	µgSi/L
21	DO	12.000	12.000	12.000	mgO2/L
22	Phytoplankton	1.000	1.000	1.000	µgA/L
23	Herb Zoo	0.00200	0.00200	0.00200	mgC/L
24	Carn Zoo	0.00200	0.00200	0.00200	mgC/L
25	Phytoplankton 2	0.000	0.000	0.000	µgA/L
26	Phytoplankton 3	0.000	0.000	0.000	µgA/L

Figure 11. The Initial Conditions worksheet.

3.2.6 Vertical Mixing Worksheet

This worksheet is used to enter information related to vertical mixing between the lake's layers (Figure 12). Two options (Mixing modes) are specified using the pull-down menu in cell b6. These are as follows (described more in Section 4.0):

1. **Munk-Anderson.** This approach employs a model to compute vertical mixing between layers based on wind speed and water density. Note that this is the default option.

2. **Time series (below).** Vertical turbulent diffusion coefficients between the layers can be entered as a time series. The program uses linear interpolation to determine the mixing coefficients between the entered dates.

	A	B	C
1	LAKE2K		
2	Lake Water Quality Model		
3	Lake Washington		
4	Vertical Mixing		
5			
6	Mixing mode	Munk-Anderson	
7	a coefficient	20.00	
8	c coefficient	5.00	
9			
10	Time Series:	Vertical Diffusion	Vertical Diffusion
11		Epi-Meta	Meta-Hypo
12	Time (d)	cm2/s	cm2/s
13	1/1/00	5.00	5.00
14	1/17/00	0.01	0.01
15	2/19/00	0.01	0.01
16	2/20/00	5.00	5.00
17	3/7/00	5.00	5.00
18	3/23/00	5.00	5.00
19	4/1/00	0.04	0.04
20	5/30/00	0.04	0.01
21	9/15/00	0.04	0.01
22	10/1/00	1.00	0.02
23	11/1/00	5.00	5.00
24	1/1/01	5.00	5.00

Figure 12. The Vertical Mixing worksheet.

Note that if the time series option is chosen, the series must encompass the simulation time series as specified in cells B16 and B17 of the LAKE2K worksheet.

3.2.7 Meteorology Worksheet

This worksheet is used to enter time series of meteorological data for the lake (Figure 13). The program uses linear interpolation to determine values between the entered dates. Note that each time series must encompass the simulation time series as specified in cells B16 and B17 of the LAKE2K worksheet. Also, note that the program internally calculates and displays values for the average daily solar radiation and the photoperiod in columns H and I.

	A	B	C	D	E	F	G	H	I
2	Lake Water Quality Model				RUN	Open Old File			
3	Onondaga Lake								
4	Met Data								
5									
6									
7		Air	Dew-Point	Wind	Cloud	Atm Turb Fac	Precip	Avg Daily	Photo
8		Temp	Temp	Speed	Cover	(2-clear)	Rate	Solar Rad	period
9	Time (d)	Ta(C)	Td(C)	Uw(mps)	C	(5-smog)	P(m/d)	(cal/cm2/d)	(hr)
10	1/1/01	-6.89	-8.67	4.53	0.50	2	0.00275	141.0	8.9
11	1/2/01	-8.98	-11.27	4.45	0.50	2	0.00275	141.9	8.9
12	1/3/01	-3.75	-9.26	5.13	0.50	2	0.00275	142.8	8.9
13	1/4/01	-3.22	-5.72	5.54	0.50	2	0.00275	143.8	8.9
14	1/5/01	-3.02	-6.06	4.03	0.50	2	0.00275	144.8	8.9

Figure 13. The Meteorological Data worksheet.

3.2.8 Ice Worksheet

This worksheet enters values that are used to compute ice thickness and to parameterize its impact on light transmission into the lake. During ice cover, the vertical turbulent dispersion coefficient is assumed to be zero (Figure 14). Details on the ice simulation are found in Section 5.0 of this document.

	A	B	C
1	LAKE2K		
2	Lake Water Quality Model		
3	Onondaga Lake		
4	Ice Parameters		
5			
6			
7	System ID:		
8	Initial thickness	0	m
9	Density of ice	916	kg/m ³
10	Latent heat of fusion of ice	334000	J/kg
11	Thermal conductivity of ice	2.24	W/(m C)
12	Heat transfer coefficient water to ice	10	W/(m ² C)
13	Snow thickness	0.05	m
14	Thermal conductivity of snow	0.2	kg/m ³
15	Light attenuation of ice	1	/m
16	Light attenuation of snow	10	/m

Figure 14. The Ice Parameters Worksheet.

3.2.9 Light and Heat Worksheet

This worksheet is used to enter information related to the lake's light regime and heat balance. Details on the heat balance are found in Section 5.0 of this document.

	A	B	C	D
1	LAKE2K			
2	Lake Water Quality Model			
3	Lake Washington			
4	Light and Heat			
5				
6	Parameter	Value	Unit	Symbol
7	Light			
8	Photosynthetically Available Radiation	0.47		
9	Forward scattering fraction	0.94	/m	γ
10	Water absorption coefficient	0.012	/m	a_w
11	Color absorption coefficient	0.5	/m	a_c
12	Chlorophyll absorption constant	0.030	m ² /mgA	a_{chl}
13	POC (as dry weight) absorption constant	0.160	m ² /gD	a_{POC}
14	Inorganic suspended solids absorption constant	0.031	m ² /gD	a_i
15	Water scattering coefficient	0.0027	/m	b_w
16	Chlorophyll scattering constant	0.010	m ² /mgA	β_{chl}
17	POC (as dry weight) scattering constant	0.240	m ² /gD	β_{POC}
18	Inorganic suspended solids scattering constant	0.370	m ² /gD	β_i
19	Heat			
20	Conduction/Evaporation constant	19		a_{UW}
21	Conduction/Evaporation wind coefficient	0.950		b_{UW}
22	Conduction/Evaporation wind power	2		c_{UW}

Figure 15. The Light and Heat Worksheet used to input light-related parameters.

3.2.10 Rates Worksheet

This worksheet is used to enter the model's rate coefficients. It consists of many entries and is broken down into several parts (Figure 16 through Figure 19). Full details about these inputs can be found in Section 6.0 of this documentation, as described in the constituent model.

	A	B	C	D
1	LAKE2K			
2	Lake Water Quality Model			
3	Lake Heiwpc			
4	Rates			
5				
6				
7	Parameter	Value	Units	Symbol
8	Stoichiometry:			
9	Dry weight	100	gD	gD
10	Carbon	40	gC	gC
11	Nitrogen	7.2	gN	gN
12	Phosphorus	1	gP	gP
13	Chlorophyll	0.8	gA	gA
14	Inorganic suspended solids:			
15	Settling velocity	0.5	m/d	v_i
16	Particulate organic carbon:			
17	Hydrolysis rate	0.05	/d	k_{hc}
18	Temperature parameter	1.07		θ_{hc}
19	Settling velocity	0.25	m/d	v_{oc}
20	Dissolved organic carbon:			
21	Oxidation rate	0.1	/d	k_{dc}
22	Temperature parameter	1.047		θ_{dc}
23	Oxygen inhibition model for DOC oxidation	Exponential		
24	Oxygen inhibition parameter	0.6	L/mgO ₂	K_{sood}

Figure 16. The part of the Rates Worksheet used to input stoichiometry and rate parameters for inorganic suspended solids, POC, and DOC.

Stoichiometry. The first section is model stoichiometry. The model assumes a fixed stoichiometry of plant and detrital matter. Recommended values for these parameters are 100 gD:40 gC:7.2 gN:1 gP : 1 gA. Chlorophyll is the most variable of these values with a range from about 0.5 to 2 gA. It is suggested that the dry weight be set to 100 gD and the other values scaled accordingly.

Inorganic suspended solids. This input defines the velocity (m/d) at which inorganic suspended solids particles settle in each layer. The velocity is size, shape, and density specific, and can be estimated using Stokes' law.

Nutrients and dissolved oxygen. These inputs control the cycling of carbon, nitrogen, phosphorus, and silica in the waterbody. Processes represented by the model include particulate carbon hydrolysis and settling, dissolved organic carbon oxidation, organic nitrogen hydrolysis and settling, nitrification, denitrification, organic phosphorus hydrolysis and settling, and dissolved oxygen reactions (sources and sinks).

Plankton. Plankton in the waterbody can be simulated by up to three phytoplankton groups (e.g., diatoms, green algae, and blue green algae) and two zooplankton groups (herbaceous and carnivorous). Coefficients controlling metabolic processes (e.g., growth rate, respiration, death), temperature limitation, nutrient limitation, and grazing of phytoplankton and zooplankton are all represented.

	A	B	C	D
25	Organic nitrogen:			
26	Hydrolysis rate	0.005	/d	k_{hn}
27	Temperature parameter	1.07		θ_{hn}
28	Settling velocity	0.035	m/d	v_{on}
29	Ammonia nitrogen:			
30	Nitrification rate	0.02	/d	k_n
31	Temperature parameter for nitrification	1.07		θ_n
32	Oxygen inhibition model for nitrification	Exponential		
33	Oxygen inhibition parameter	0.6	L/mgO ₂	K_{sona}
34	Nitrate nitrogen:			
35	Denitrification rate	0.05	/d	k_{dn}
36	Temperature parameter for denitrification	1.07		θ_{dn}
37	Oxygen trigger model for denitrification	Exponential		
38	Oxygen trigger	0.6	L/mgO ₂	K_{sodn}
39	Carbon half saturation constant	0.05	mgC/L	K_{sloc}
40	Organic phosphorus:			
41	Hydrolysis rate	0.007	/d	k_{hp}
42	Temperature parameter for organic P hydrolysis	1.07		θ_{hp}
43	Settling velocity	0.05	m/d	v_{op}
44	Organic silica:			
45	Dissolution	0.03	/d	k_{hs}
46	Temperature parameter for organic Si hydrolysis	1.07		θ_{hs}
47	Settling velocity	0.25	m/d	v_{os}
48	Dissolved oxygen:			
49	Temperature parameter for reaeration	1.024		θ_{oc}
50	Oxygen per C oxidized	2.67	gO ₂ /gC	r_{oc}
51	Oxygen per N nitrified	4.57	gO ₂ /gN	r_{on}
52	Reaeration formula	O'Connor		

Figure 17. The part of the Rates Worksheet used to input parameters for organic nitrogen, ammonia nitrogen, nitrate nitrogen, organic phosphorus, organic silica, and dissolved oxygen.

53	Phytoplankton:	Phytoplankton 1		Phytoplankton 2		Phytoplankton 3	
54	Maximum growth rate	3.5 /d	k_{gp}	0 /d	k_{gp}	0 /d	k_{gp}
55	Temperature model for growth	Optimal	θ_{gp}	Arrhenius(Theta)	θ_{gp}	Arrhenius(Theta)	θ_{gp}
56	Theta or Topt	10 C	k_{gp}	1.066	k_{gp}	1.066	k_{gp}
57	Kappa1	0.005	θ_{gp}	0	θ_{gp}	0.005	θ_{gp}
58	Kappa2	0.01	θ_{gp}	0	θ_{gp}	0.005	θ_{gp}
59	Respiration rate	0.025 /d	k_{rp}	0.05 /d	k_{rp}	0.15 /d	k_{rp}
60	Temperature parameter for respiration	1.07	θ_{rp}	1.07	θ_{rp}	1.07	θ_{rp}
61	Death rate	0.025 /d	k_{dp}	0 /d	k_{dp}	0 /d	k_{dp}
62	Temperature parameter for death	1.08	θ_{dp}	1.08	θ_{dp}	1.08	θ_{dp}
63	Nitrogen half saturation	25 µgN/L	K_{sn}	2 µgN/L	K_{sn}	25 µgN/L	K_{sn}
64	Phosphorus half saturation	5 µgP/L	K_{sp}	2 µgP/L	K_{sp}	2 µgP/L	K_{sp}
65	Silica half saturation	50 µgSi/L	K_{ss}	0 µgSi/L	K_{ss}	0 µgSi/L	K_{ss}
66	Light model	Steele		Steele		Steele	
67	Light parameter	250 langleys/d	k_{si}	350 langleys/d	k_{si}	300 langleys/d	k_{si}
68	Settling velocity	0.2 m/d	v_s	0.05 m/d	v_s	0.1 m/d	v_s
69	Ammonia preference parameter	25 µgN/L	P_{sm}	25 µgN/L	P_{sm}	25 µgN/L	P_{sm}
70	Grazability	1	F_g	0	F_g	1	F_g
71	Silica content	24 gSi	gSi	0 gSi	gSi	0 gSi	gSi

Figure 18. The part of the Rates Worksheet used to input rate parameters for up to three phytoplankton assemblages.

72	Herbivorous Zooplankton:		
73	Maximum grazing rate	3 m3/gC/d	C_{gh}
74	Temperature parameter for grazing	1.07	θ_{gh}
75	Respiration rate	0.1 /d	k_{rh}
76	Temperature parameter for respiration	1.07	θ_{rh}
77	Death rate	0 /d	k_{dh}
78	Temperature parameter for death	1.07	θ_{dh}
79	Grazing efficiency	0.6	e_h
80	Algae half saturation constant	10 ugA/L	k_{sa}
81	Carnivorous Zooplankton:		
82	Maximum grazing rate	2 m3/gC/d	C_{gc}
83	Temperature parameter for grazing	1.07	θ_{gc}
84	Respiration rate	0.1 /d	k_{rc}
85	Temperature parameter for respiration	1.07	θ_{rc}
86	Death rate	0.05 /d	k_{dc}
87	Temperature parameter for death	1.07	θ_{dc}
88	Grazing efficiency	0.6	e_c
89	Herbivore half saturation constant	0 mgC/L	k_{sh}

Figure 19. The part of the Rates Worksheet used to input rate parameters for herbivorous and carnivorous zooplankton.

3.3 DATA WORKSHEETS

These worksheets are used to enter measured data that is displayed on plots. As such, they are optional. They are distinguished by pale yellow tabs.

Note that this data can be arranged in any order. However, no blank rows should be included. If the program encounters a blank row below the first row, all data in lower rows will not be saved when the program is run.

3.3.1 Physical Data Worksheet

This worksheet is used to enter a time series of measured lake depths and solar radiation as a function of date (Figure 20).

	A	B	C	D
1	LAKE2K			
2	Lake Water Quality Model			
3	Lake Neiwpc			
4	Data: Physical			
5				
6				
7		Depth		Solar
8	t (d)	(m)	t (d)	(ly/d)
9				
10				
11				
12				
13				
14				

Figure 20. The Physical Data Worksheet.

3.3.2 Water Quality Data Worksheets

There are three worksheets that are used to enter model data for water quality in the epilimnion, metalimnion, and hypolimnion. Figure 21 shows the epilimnion data sheet.

	A	B	C	D	E	F
1	LAKE2K					
2	Lake Water Quality Model					
3	Lake Nalms					
4	Data: Epilimnion					
5						
6						
7		T-epi	Cond-epi	ISS-epi	POC-epi	DOC-epi
8	t (d)	Data	Data	Data	Data	Data
9	1/15/93	4.00				
10	2/15/93	5.00				
11	3/15/93	6.00				
12	4/15/93	8.50				
13	5/15/93	13.00				

Figure 21. The Epilimnion Data Worksheet.

3.3.3 Miscellaneous Data Worksheet

This worksheet is used to enter data for Secchi depths and light extinction coefficients (Figure 22).

	A	B	C
1	LAKE2K		
2	Lake Water Quality Model		
3	Onondaga Lake		
4	Data: Miscellaneous		
5			
6			
7		SD	ke
8	t (d)	(m)	(/m)
9	4/5/01	1.10	
10	4/9/01	0.40	2.27
11	4/16/01	0.90	1.23
12	4/23/01	1.60	1.01
13	4/30/01	0.75	1.09
14	5/7/01	1.20	0.96
15	5/14/01	1.50	1.02

Figure 22. The Miscellaneous Data Worksheet.

3.4 Output Worksheets

Output is presented in the form of numerical time series output tables generated by L2K. Most of this information is displayed in graphical form in subsequent charts as will be described in Section 3.5. These worksheets are distinguished by pale green tabs.

Hydraulics Output Worksheet. This worksheet summarizes the flow, precipitation, volume, depth, and ice thickness time series computed by the model (Figure 23).

	A	B	C	D	E	F
1	LAKE2K					
2	Lake Water Quality Model					
3	Lake Halms					
4	Output: Hydraulics					
5						
6						
7						
8						
9	t (hr)	Qin (m3/s)	Qout (m3/s)	Vol (m3)	Depth (m)	Ice Thickness (m)
10	1/1/93	0.93	0.74	48966156	26.27	0.00
11	1/6/93	0.94	0.74	49047433	26.29	0.96
12	1/11/93	0.93	0.74	49139863	26.31	1.88
13	1/16/93	0.91	0.74	49223876	26.33	2.46
14	1/21/93	0.89	0.74	49297420	26.35	2.68
15	1/26/93	0.87	0.74	49360635	26.37	2.57

Figure 23. The Hydraulics Output Worksheet.

Water Quality Variables Output Worksheet. This worksheet presents the time series of all the model variables for each layer of the lake (Figure 24).

	A	B	C	D	E	F	G
1	LAKE2K						
2	Lake Water Quality Model				RUN	Open Old File	
3	Onondaga Lake						
4	Output: WQ Variables						
5							
6							
7							
8		Temperature (C)			Specific Conductance (umhos)		
9	t (hr)	T-epi	T-meta	T-hypo	Cond-epi	Cond-meta	Cond-hypo
10	1/1/01	0.00	0.50	1.00	2250.00	2250.00	2250.00
11	1/2/01	0.02	0.51	1.03	2248.89	2250.07	2254.42
12	1/3/01	0.03	0.52	1.06	2247.73	2250.27	2258.57
13	1/4/01	0.04	0.53	1.10	2246.61	2250.59	2262.19
14	1/5/01	0.05	0.54	1.13	2245.53	2251.00	2265.08
15	1/6/01	0.06	0.55	1.16	2244.48	2251.46	2267.82
16	1/7/01	0.07	0.57	1.19	2243.48	2251.97	2270.28

Figure 24. The WQ Variables Output Worksheet.

Miscellaneous Output. This worksheet presents the time series of miscellaneous variables that are computed by L2K. As in Figure 25, quantities include the DO saturation of the epilimnion as well as the total phosphorus, total nitrogen and total silica concentrations for all three layers and the lake as a whole. The total phytoplankton and total suspended solids concentrations are displayed for each layer. In addition, computed Secchi depths and light extinction coefficients are listed.

	A	B	C	D	E	F	G	H	I
1	LAKE2K								
2	Lake Water Quality Model				RUN	Open Old File			
3	Lake Washington								
4	Output Miscellaneous								
5									
6									
7									
8									
9	t (d)	DO-sat	TP-epi	TP-meta	TP-hypo	TP-Lake	TN-epi	TN-meta	TN-hypo
10	1/1/95	11.83	20.60	20.60	20.60	20.60	374.32	374.32	374.32
11	1/6/95	12.01	20.79	20.79	20.79	20.79	376.19	376.13	376.12
12	1/11/95	12.04	20.89	20.89	20.85	20.87	377.81	377.68	377.05
13	1/16/95	12.07	20.96	20.95	20.95	20.95	378.82	378.78	378.75
14	1/21/95	12.12	21.04	21.04	21.04	21.04	379.96	379.92	379.90
15	1/26/95	12.17	21.09	21.08	21.08	21.08	380.63	380.61	380.60
16	1/31/95	12.08	21.25	21.23	21.12	21.17	382.90	382.55	381.15
17	2/5/95	12.00	21.40	21.38	21.19	21.27	389.73	388.28	382.41
18	2/10/95	12.06	21.26	21.26	21.26	21.26	388.95	388.87	385.23

Figure 25. The Miscellaneous Variable Worksheet.

Heat Output Worksheet. This worksheet presents the time series of the heat budget, including solar shortwave, atmospheric longwave, back radiation, sensible, and latent heat transfer.

Sediment-Water Variables Output Worksheet. This worksheet presents the time series of sediment-water variables that correspond to the sediments beneath each layer. These include SOD and nutrient fluxes. Note that a positive SOD signifies a loss of oxygen from the layer to the sediments. In contrast, a positive nutrient flux signifies a transfer of nutrients from the sediments to the water.

	A	B	C	D	E	F	G	H
1	LAKE2K							
2	Lake Water Quality Model							
3	Lake Nalms				RUN	Open Old File		
4	Output Sediment Fluxes							
5								
6								
7								
8	time	EPI SOD	EPI JNH4	EPI JN03	EPI JP04	EPI JCH4	META SOD	META JNH4
9	(day)	gO2/m2/d	mgN/m2/d	mgN/m2/d	mgP/m2/d	gO2/m2/d	gO2/m2/d	mgN/m2/d
10	1/1/93	0.06	0.04	-0.12	0.05	0.00	0.06	0.04
11	1/6/93	0.06	0.03	-0.12	0.05	0.00	0.06	0.02
12	1/11/93	0.06	0.01	-0.12	0.05	0.00	0.06	0.01
13	1/16/93	0.06	0.00	-0.13	0.04	0.00	0.06	-0.01
14	1/21/93	0.06	-0.01	-0.14	0.04	0.00	0.06	-0.02
15	1/26/93	0.06	-0.03	-0.15	0.04	0.00	0.06	-0.04
16	1/31/93	0.06	-0.04	-0.16	0.03	0.00	0.06	-0.05
17	2/5/93	0.06	-0.05	-0.18	0.03	0.00	0.06	-0.06

Figure 26. The Sediment Flux Output Worksheet.

3.5 Output Charts

Along with the tabular output, there are numerous charts that display model output graphically. These are all clustered after the tabular output and are indicated with pale pink tabs:

Output Heat	Output Seds	Air Dew Point Plot	Solar Photo Plot	FI
-------------	-------------	--------------------	------------------	----

We have tried to make these plots self-explanatory by including a yellow key at the bottom. The Temperature Plot (Figure 27) displays the temperature time series for the three layers along with ice thickness. As described in the key, the model predictions are represented with different colored lines and the measured data with different shaped symbols with colors corresponding to the lines. Because the temperatures use a different scale than the ice thickness, a secondary scale is used for the latter.

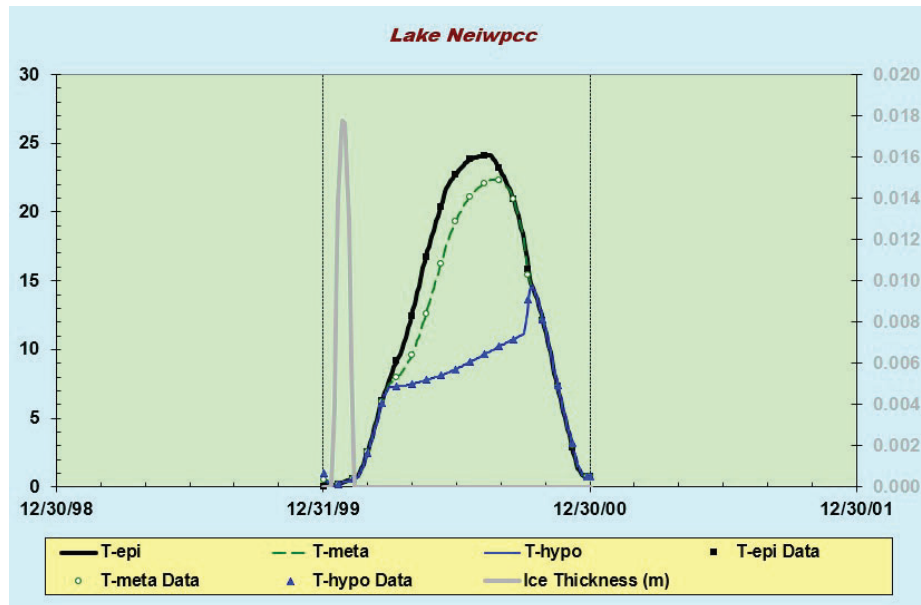



Figure 27. The Temperature Plot which displays the temperatures of the three layers along with ice thickness. As described by the key, the model predictions are

represented with different colored lines and the measured data with different shaped symbols with the same colors as the lines.

3.6 Navigating the Sheets and Charts

Because there are so many sheets and charts, it can be cumbersome selecting the ones you desire. A neat trick to do that is to place the mouse pointer on the  button at the bottom left of the Excel screen and right click. As illustrated in Figure 28, an activation window will open listing all the sheets and charts in Lake2K. Then, by selecting your desired target, you will immediately jump to that sheet or chart.

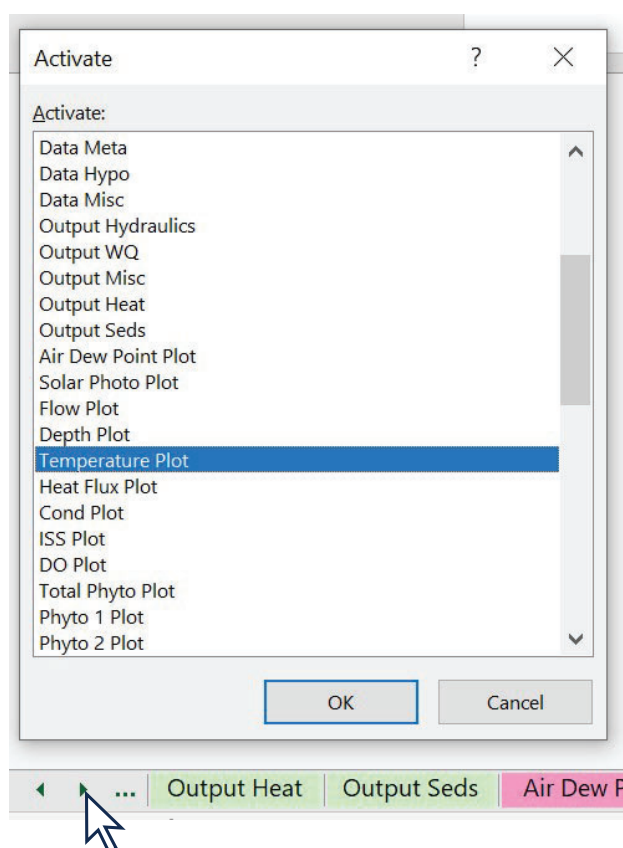


Figure 28. How to jump to any sheet or chart by positioning the mouse pointer on the  arrow on the lower left corner of the Excel screen.

Part II

Documentation

This section provides a description of the model theory.

4 PHYSICS

The model presently simulates the lake as a one-dimensional system consisting of three vertical layers (Figure 29). The volumes of the two deeper layers (metalimnion and hypolimnion) are held fixed whereas the epilimnion is allowed to change as a function of the balance between inflows and outflows.

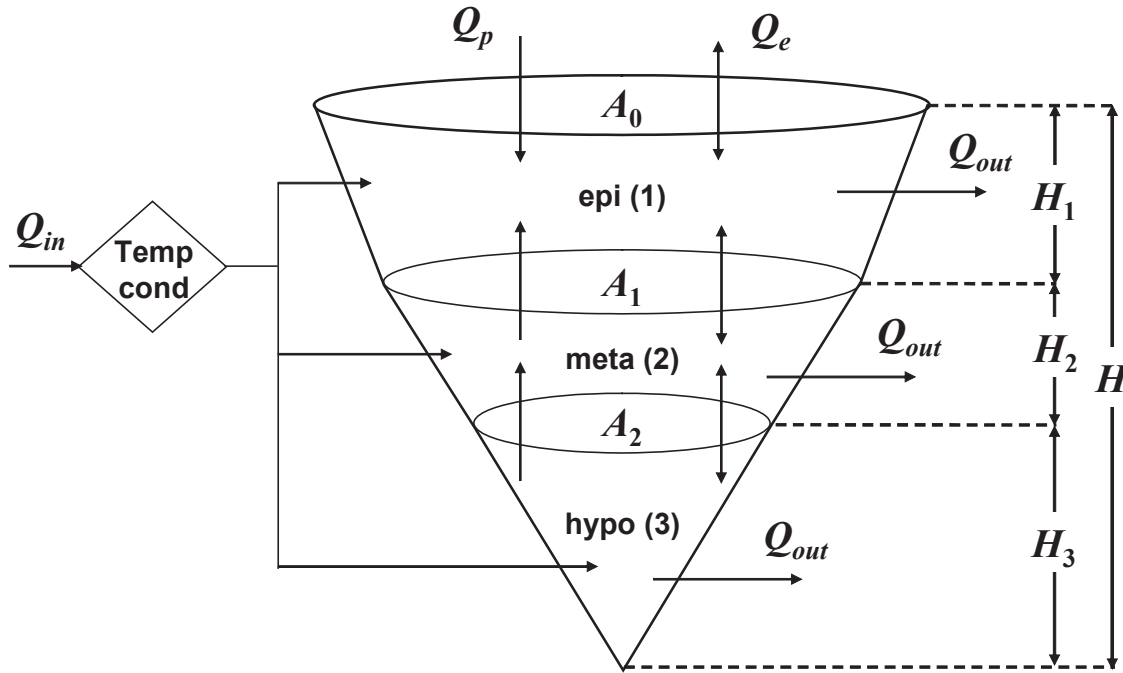


Figure 29 LAKE2K water balance and vertical segmentation scheme.

The inflow is routed into one of the layers depending on the density of the inflow and the layer according to the algorithm:

- If the inflow density is less than the average of the epilimnion and metalimnion densities, the inflow enters the epilimnion.
- If the inflow density is greater than the average of the metalimnion and hypolimnion densities, the inflow enters the hypolimnion.
- Otherwise, the inflow enters the metalimnion.

If necessary (that is, if the flow enters the hypolimnion or metalimnion), the flow is routed through the other layers and exits through either the epilimnion or the hypolimnion depending on the user's choice of outflow mode. The density is related to water temperature and dissolved solids by an equation of state as described in Appendix A.

4.1 Water Balance

A dynamic water balance is computed for the overall volume of the lake as in

$$\frac{dV}{dt} = Q_{in} + Q_p - Q_e - Q_{out} \quad (1)$$

where V = lake volume [m^3], t = time (d), Q_{in} = inflow [m^3/d], Q_p = precipitation volume [m^3/d], Q_e = evaporation flow [m^3/d], and Q_{out} = outflow [m^3/d]. This equation is integrated to simulate how the lake's volume changes as a function of time. Each term in the balance is described next.

4.1.1 Inflow

The inflow represents the sum of all the flows entering the lake from tributaries, and direct point and nonpoint sources. The user enters these values as a single time series of dates and flows.

4.1.2 Precipitation

Precipitation flow is entered as a time series of dates and precipitation rates. The program then computes the precipitation flow as

$$Q_p = PA_0 \quad (2)$$

where P = the precipitation rate [m/d], and A_0 = the lake's surface area [m^2/d].

4.1.3 Evaporation

The model internally computes the loss of water due to evaporation. This flow is computed as

$$Q_e = \frac{J_e A_0}{\rho L_e} \times \frac{\text{m}}{100 \text{ cm}} \quad (3)$$

where J_e = the heat flux due to evaporation [$\text{cal}/\text{cm}^2/\text{d}$], ρ = the density of water [$=1 \text{ g}/\text{cm}^3$], and L_e = the latent heat of vaporization [cal/g]. The latent heat is related to temperature by

$$\frac{dV}{dt} = Q_{in} + Q_p - Q_e - Q_{out} \quad (4)$$

where T_1 = the temperature of the epilimnion [$^{\circ}\text{C}$]. The heat flux lost due to evaporation is computed as a function of wind speed, the dew-point temperature and the epilimnion temperature as described below in Sec. 5.1.5.

4.1.4 Outflow

Seven options are available to compute outflow. The desired method is chosen using the pull-down menu in cell B6 on the Outflow worksheet (Figure 10).

- **Flowout(epi)=Flowin.** The outflow is set equal to the inflow. For this case, the outflow exits the lake from the epilimnion. Note that if the Outflow Mode is left blank, this is the default option.

- **Flowout(meta)=Flowin.** The outflow is set equal to the inflow. For this case, the outflow exits the lake from the metalimnion.
- **Flowout(hypo)=Flowin.** The outflow is set equal to the inflow. For this case, the outflow exits the lake from the hypolimnion.
- **Time Series (epi).** The user can enter a time series of outflows into columns A and B. The program uses linear interpolation to determine values between the entered dates. For this case, the outflow exits the lake from the epilimnion.
- **Time Series (meta).** The user can enter a time series of outflows into columns A and B. The program uses linear interpolation to determine values between the entered dates. For this case, the outflow exits the lake from the metalimnion.
- **Time Series (hypo).** The user can enter a time series of outflows into columns A and B. The program uses linear interpolation to determine values between the entered dates. For this case, the outflow exits the lake from the hypolimnion.
- **Stage-Discharge.** The user can enter a stage-discharge curve in tabular form in columns D and E. The program uses linear interpolation to determine intermediate values.

Note that if any of the time series options are chosen the series must encompass the simulation time series as specified in cells B16 and B17 of the LAKE2K worksheet.

4.2 Vertical Segmentation and Mixing

The lake is divided vertically into three layers as depicted in Figure 29. The model uses turbulent diffusion to mix water between the layers. For a conservative substance with no flow, a mass balance for the metalimnion can be written as

$$\frac{dc_2}{dt} = \frac{E'_1}{V_2}(c_1 - c_2) + \frac{E'_2}{V_2}(c_3 - c_2) \quad (5)$$

where c_i = the concentration in layer i [g/m³], $i = 1, 2$, and 3 for the epi-, meta- and hypolimnion, respectively, E'_i = the bulk turbulent diffusion coefficient across the lower boundary of layer i [m³/d], and V_i = the volume of layer i [m³]. The bulk dispersion coefficient is related to more fundamental quantities by

$$E'_i = \frac{E_i A_i}{(H_i + H_{i+1})/2} \quad (6)$$

where E_i = the turbulent diffusion coefficient across the lower boundary of layer i [m²/d], A_i = the surface area of the boundary of layer i [m²], and H_i = the thickness of layer i [m] (see Figure 29).

Two options (Mixing modes) are available to determine the turbulent diffusion coefficients as specified using the pull-down menu in cell B6 of the Vertical Mixing Worksheet (Figure 12). These are:

Munk-Anderson. This approach employs a model to compute vertical mixing between layers based on wind speed and water density developed originally by Munk and Anderson (1948). The vertical turbulent diffusion coefficient is computed as

$$E = \frac{E_0}{(1 + aR_i)^{0.5}} \quad (7)$$

where E_0 = the maximum diffusion coefficient [m^2/d], a = a tuning coefficient, and R_i = the Richardson number.

The maximum diffusion coefficient is proportional to the shear velocity (Sundaram and Rehm 1973),

$$E_0 = cU^* \quad (8)$$

where c = a tuning coefficient and U^* = the shear velocity [m/s]. The shear velocity is computed as

$$U^* = \sqrt{\frac{\rho_{\text{air}} C_d U_w^2}{\rho}} \quad (9)$$

where ρ_{air} = the density of the air (assumed equal to 1.2 kg/m^3), C_d = a dimensionless drag coefficient (assumed equal to 1.3×10^{-3}), U_w = the wind speed [m/s], and ρ = the density of the water [kg/m^3]. In our case, ρ is the density of the water in the lake's epilimnion.

The Richardson number is a dimensionless number that represents the ratio of buoyancy to shear forces. Ford and Johnson (1986) have proposed the following formula to compute the Richardson number,

$$R_i = -\frac{(g/\rho)(\partial\rho/\partial z)}{U^*/(z_s - z)^2} \quad (10)$$

where g = the acceleration due to gravity ($= 9.81 \text{ m/s}^2$), ρ = the water density at the depth at which the Richardson number is computed [kg/m^3], $\partial\rho/\partial z$ = the gradient of density with depth, z_s = the water surface elevation and z = the elevation at which the Richardson number is computed [m].

The density gradient at the interface between layers is computed with a finite divided difference

$$\frac{\partial\rho}{\partial z} = \frac{\rho_i - \rho_{i+1}}{z_i - z_{i+1}} \quad (11)$$

where ρ_i = the density for layer i [kg/m^3] and z_i = the elevation at the midpoint of layer i [m].

The model is tuned by adjusting the coefficients a and c until there is an acceptable match between simulated and measured temperatures for each model layer. The default value for a is 30 with a range from 10 to 60. A default value for c is estimated as

$$c = \frac{H_{\max}}{34} \quad (12)$$

where H_{\max} = the maximum depth of the lake [m].

Time series (below). Vertical turbulent diffusion coefficients between the layers can be entered as a time series. The program uses linear interpolation to determine the mixing coefficients between the entered dates.

5 TEMPERATURE MODEL

A heat balance is written for each vertical layer. For the epilimnion for the case where the inflow and outflow pass through the epilimnion and there is no ice cover, the balance is written as

$$\begin{aligned} \frac{dHeat_1}{dt} = & Q_{in} \rho C_p T_{in} \left(\frac{10^6 \text{ cm}^3}{\text{m}^3} \right) + Q_p \rho C_p T_{air} \left(\frac{10^6 \text{ cm}^3}{\text{m}^3} \right) - Q_{out} \rho C_p T_1 \left(\frac{10^6 \text{ cm}^3}{\text{m}^3} \right) \\ & + E'_1 \rho C_p (T_2 - T_1) \left(\frac{10^6 \text{ cm}^3}{\text{m}^3} \right) + J_h A_0 \left(\frac{10^4 \text{ cm}^2}{\text{m}^2} \right) \end{aligned} \quad (13)$$

where $Heat_1$ = heat of the epilimnion [cal], t = time [d], ρ = the density of water [g/cm^3], C_p = the specific heat of water [$\text{cal}/(\text{g } ^\circ\text{C})$], T_{in} = temperature of the inflow [$^\circ\text{C}$], T_i = temperature in layer i [$^\circ\text{C}$], T_{air} = air temperature [$^\circ\text{C}$], E'_i = the bulk dispersion coefficient across the lower boundary of layer i [m^3/d], A_i = the area at the bottom of layer i [m^2], and J_h = the air-water heat flux [$\text{cal}/(\text{cm}^2 \text{ d})$]. Similar balances are written for the other layers with the noteworthy exception that the surface heat flux is omitted.

5.1 Surface Heat Flux

As depicted in Figure 30, surface heat exchange is modeled as a combination of five processes:

$$J_h = I(0) + J_{an} - J_{br} - J_c - J_e \quad (14)$$

where $I(0)$ = net solar shortwave radiation at the water surface, J_{an} = net atmospheric longwave radiation, J_{br} = longwave back radiation from the water, J_c = conduction, and J_e = evaporation. All fluxes are expressed as $\text{cal}/\text{cm}^2/\text{d}$.

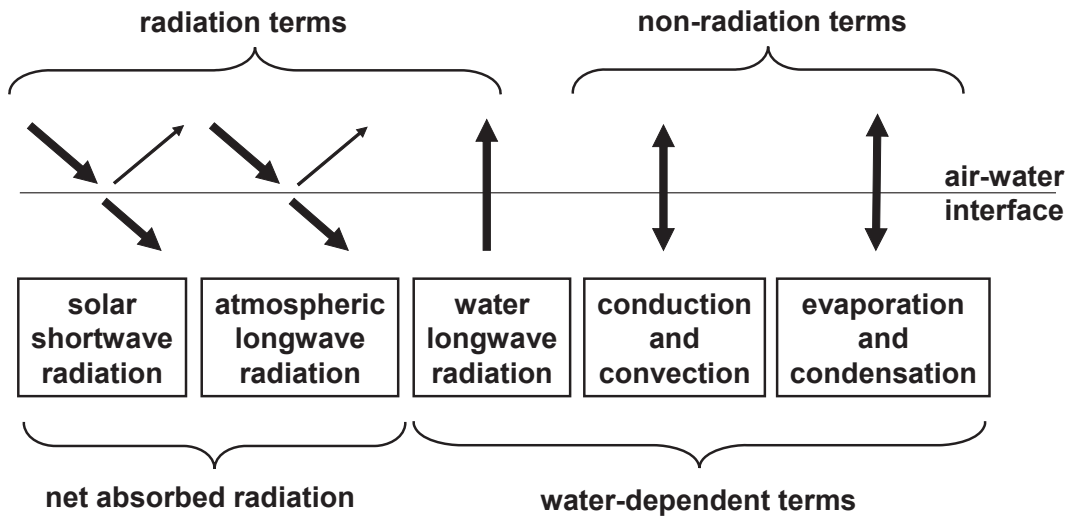


Figure 30 Components of surface heat exchange.

5.1.1 Solar Radiation

The model computes the amount of solar radiation entering the water at a particular latitude (L_{at}) on the earth's surface. This quantity is a function of the radiation at the top of the earth's atmosphere which is attenuated by atmospheric transmission, cloud cover, and reflection,

$$I(0) = I_0 a_t a_c (1 - R_s) \quad (15)$$

extraterrestrial radiation atmospheric attenuation cloud attenuation reflection

where $I(0)$ = solar radiation at the water surface [cal/cm²/d], I_0 = extraterrestrial radiation (i.e., at the top of the earth's atmosphere) [cal/cm²/d], a_t = atmospheric attenuation, C_L = fraction of sky covered with clouds, and R_s = albedo (fraction reflected).

Extraterrestrial radiation. The extraterrestrial radiation is computed as (TVA 1972)

$$I_0 = \frac{W_0}{r^2} \sin \alpha \quad (16)$$

where W_0 = the solar constant [1367 W/m² or 2823 cal/cm²/d], r = normalized radius of the earth's orbit (i.e., the ratio of actual earth-sun distance to mean earth-sun distance), and α = the sun's altitude [radians], which can be computed as

$$\sin \alpha = \sin \delta \sin L_{at} + \cos \delta \cos L_{at} \quad (17)$$

where δ = solar declination [radians], and L_{at} = local latitude [radians].

The normalized radius can be estimated as

$$r = 1 + 0.017 \cos\left(\frac{2\pi}{365}(186 - Dy)\right) \quad (18)$$

where Dy = Julian day (Jan. 1 = 1, Jan. 2 = 2, etc.).

The solar declination can be estimated as

$$\delta = 23.45 \frac{\pi}{180} \cos\left(\frac{2\pi}{365}(172 - Dy)\right) \quad (19)$$

The photoperiod f [hours] is computed as

$$f = \frac{2}{(15)24} \frac{180}{\pi} \left[\arctan\left(\frac{L}{\sqrt{1 - L \times L}}\right) + 2 \arctan(1) \right] \quad (20)$$

where

$$L = -\tan\left(\frac{\pi}{180}\delta\right)\tan(L_{at}) \quad (21)$$

Atmospheric attenuation. Various methods have been published to estimate the fraction of the atmospheric attenuation from a clear sky (a_t). L2K uses the method developed by Bras (1990),

$$a_t = e^{-n_{fac}a_1m} \quad (22)$$

where n_{fac} is an atmospheric turbidity factor that varies from approximately 2 for clear skies to 4 or 5 for smoggy urban areas. The molecular scattering coefficient (a_1) is calculated as

$$a_1 = 0.128 - 0.054 \log_{10} m \quad (23)$$

where m is the optical air mass, calculated as

$$m = \frac{1}{\sin \alpha + 0.15(\alpha_d + 3.885)^{-1.253}} \quad (24)$$

where α_d is the sun's altitude in degrees from the horizon = $\alpha \times (180^\circ/\pi)$.

Cloud Attenuation. Attenuation of solar radiation due to cloud cover is computed with

$$a_c = 1 - 0.65C_L^2 \quad (25)$$

where C_L = fraction of the sky covered with clouds.

Reflectivity. Reflectivity is calculated as

$$R_s = A\alpha_d^B \quad (26)$$

where A and B are coefficients related to cloud cover (Table 1).

Table 1 Coefficients used to calculate reflectivity based on cloud cover.

Cloudiness	Clear		Scattered		Broken		Overcast	
C_L	0		0.1-0.5		0.5-0.9		1.0	
Coefficients	A	B	A	B	A	B	A	B
	1.18	-0.77	2.20	-0.97	0.95	-0.75	0.35	-0.45

5.1.2 Atmospheric Long-wave Radiation

The downward flux of longwave radiation from the atmosphere is one of the largest terms in the surface heat balance. This flux can be calculated using the Stefan-Boltzmann law

$$J_{an} = \sigma(T_{air} + 273)^4 \varepsilon_{sky} (1 - R_L) \quad (27)$$

where σ = the Stefan-Boltzmann constant = 11.7×10^{-8} cal/(cm² d K⁴), T_{air} = air temperature [°C], ε_{sky} = effective emissivity of the atmosphere [dimensionless], and R_L = longwave reflection coefficient [dimensionless]. Emissivity is the ratio of the longwave radiation from an object compared with the radiation from a perfect emitter at the same temperature. The reflection coefficient, R_L , is generally small and is typically assumed to equal 0.03. The effective emissivity is computed with

$$\varepsilon_{sky} = A_a + A_b \sqrt{e_{air}} \quad (28)$$

where A_a and A_b are empirical coefficients, and e_{air} = the air vapor pressure [in mm Hg], which is computed as (Raudkivi 1979):

$$e_{air} = 4.596e^{\frac{17.27T_d}{237.3+T_d}} \quad (29)$$

where T_d = the dew-point temperature [°C]. Values of A_a have been reported to range from about 0.5 to 0.7 and values of A_b have been reported to range from about 0.031 to 0.076 mmHg^{-0.5} for a wide range of atmospheric conditions. LAKE2K uses a default mid-range value of $A_a = 0.6$ with $A_b = 0.031$ mmHg^{-0.5}.

5.1.3 Water Long-wave Radiation

The back radiation from the water surface is represented by the Stefan-Boltzmann law,

$$J_{br} = \varepsilon \sigma (T_1 + 273)^4 \quad (30)$$

where ε = emissivity of water (= 0.97) and T = the water temperature [°C].

5.1.4 Conduction and Convection

Conduction is the transfer of heat from molecule to molecule when matter of different temperatures are brought into contact. Convection is heat transfer that occurs due to mass movement of fluids. Both can occur at the air-water interface and can be described by,

$$J_c = c_1 f(U_w) (T_1 - T_{air}) \quad (31)$$

where c_1 = Bowen's coefficient (= 0.47 mmHg/°C). The term, $f(U_w)$, defines the dependence of the transfer on wind velocity over the water surface where U_w is the wind speed measured a fixed distance above the water surface.

There are a variety of formulas that have been proposed to define the wind dependence conduction/convection (and evaporation). The following form is used in L2K,

$$f(U_w) = a_{Uw} + b_{Uw} U_w^{c_{Uw}} \quad (32)$$

where U_w = wind speed at a height of 7 m [m/s], and a_{U_w} , b_{U_w} and c_{U_w} are user-specified coefficients. If the user leaves these values blank, the coefficients default to the relationship that was proposed by Brady, Graves and Geyer (1969) based on data from cooling ponds,

$$f(U_w) = 19.0 + 0.95U_w^2 \quad (33)$$

The height of wind speed measurements is also an important consideration for estimating conduction/convection and evaporation. The input values for wind speed (Figure 13) are assumed to be representative of conditions at a height of 7 meters above the water surface. To convert wind speed measurements ($U_{w,z}$ in m/s) taken at any height (z_w in meters) to the equivalent conditions at a height of 7 m, the exponential wind law equation may be used (TVA, 1972):

$$U_w = U_{wz} \left(\frac{z}{z_w} \right)^{0.15} \quad (34)$$

For example, if wind speed data were collected from a height of 2 m, then the wind speed at 7 m for input to the **Meteorology** worksheet (Figure 13) would be estimated by multiplying the measured wind speed by a factor of 1.2.

5.1.5 Evaporation and Condensation

The heat loss due to evaporation can be represented by Dalton's law,

$$J_e = f(U_w)(e_s - e_{air}) \quad (35)$$

where e_s = the saturation vapor pressure at the water surface [mmHg], which is computed as

$$e_s = 4.596e^{\frac{17.27T_1}{237.3+T_1}} \quad (36)$$

and e_{air} = the air vapor pressure of the overlying air [mmHg] as computed with Eq. (29).

5.2 Ice Model

The model computes ice thickness using a heat balance written at the air-water interface (Figure 31). The result is the following differential equation for ice thickness (Ashton 1986),

$$\frac{dh_i}{dt} = \frac{1}{\rho_i L_f} \left[- \frac{1}{h_i / k_i + h_s / k_s + 1 / H_{ia}} T_a - H_{wi} T_1 \right] \times \frac{86,400 \text{ s}}{d} \quad (37)$$

where h_i = ice thickness [m], ρ_i = ice density [kg/m³], L_f = latent heat of fusion of ice [J/kg], k_i = ice thermal conductivity [W/(m °C)], h_s = snow thickness [m], k_s = snow thermal conductivity [W/(m °C)], H_{ia} = heat transfer coefficient between ice and atmosphere [W/(m² °C)], and H_{wi} = heat transfer coefficient between water and ice [W/(m² °C)]. Recommended values for several of the model parameters are listed in Table 2.

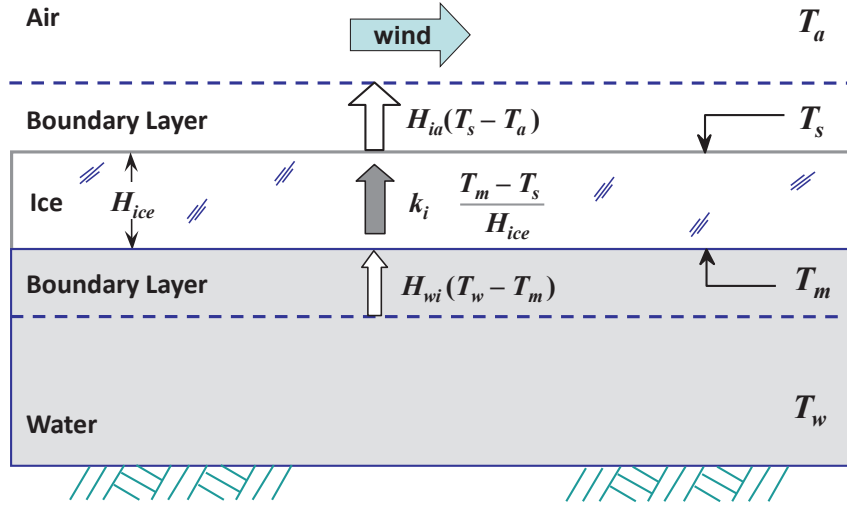


Figure 31 Components of surface heat exchange.

The heat transfer coefficient between the ice and the atmosphere is a function of the wind velocity (Martin and McCutcheon 1999),

$$H_{ia} = 5.7 + 3.8U_w \quad (38)$$

Table 2 Recommended values for ice parameters

Parameter	Symbol	Value	Units
ice thermal conductivity	k_i	2.24	W/(m °C)
snow thermal conductivity	k_s	0.2	W/(m °C)
ice density	ρ_i	916	kg/m ³
latent heat of fusion for ice	L_f	334,000	J/kg

Both the snow thickness and the heat transfer coefficient between the water and ice varies considerably from system to system and are considered tuning parameters in the present version of the model. Snow acts as an insulator that retards heat transfer between the ice and the atmosphere. The water-ice heat transfer coefficient detracts from the rate of ice formation.

Equation (37) is integrated to determine ice thickness. If ice is formed, several model mechanisms are modified:

Surface heat flux. The atmospheric heat flux is set to zero and is replaced by the heat transfer from the water to the ice. Thus, Eq. (13) becomes

$$\frac{dHeat_1}{dt} = [\text{Flow \& Dispersion Terms}] - H_{wi}A_0T_1 \times \frac{\text{cal}}{4.1868 \text{ J}} \times \frac{86,400 \text{ s}}{\text{d}} \quad (39)$$

Evaporative water loss. An impact of atmospheric heat flux being set to zero is that the loss of water via evaporation does not occur [that is, $J_e = 0$ in Eq. (14)].

Gas transfer. In the presence of ice, the model automatically sets the oxygen mass transfer rate to zero.

Light penetration. Light penetration is affected by ice and snow cover. The Beer-Lambert law is used to compute this reduction as in

$$PAR(0) = PAR_{is} e^{-K_{di}h_i - K_{ds}h_s} \quad (40)$$

where $PAR(0)$ = the mean daytime photosynthetically available radiation (PAR) at the water surface [ly/d], PAR_{is} = the PAR at the top of the ice-snow layer [ly/d], K_{di} = the ice light extinction coefficient [m^{-1}], and K_{ds} = the snow light extinction coefficient [m^{-1}].

Vertical mixing. The presence of ice greatly diminishes vertical turbulent diffusion. At present, the model sets the values of the vertical diffusion coefficients to zero to reflect this impact (Figure 12)

6 CONSTITUENT MODEL

6.1 Constituents and General Mass Balance

The model constituents are listed in Table 3.

Table 3 Model state variables

Variable	Symbol	Units*
Conductivity	s	μmhos
Inorganic suspended solids	m_i	mgD/L
Dissolved oxygen	o	mgO_2/L
Particulate organic carbon	c_p	mgC/L
Dissolved organic carbon	c_f	mgC/L
Organic nitrogen	n_o	$\mu\text{gN/L}$
Ammonia nitrogen	n_a	$\mu\text{gN/L}$
Nitrate nitrogen	n_n	$\mu\text{gN/L}$
Organic phosphorus	p_o	$\mu\text{gP/L}$
Inorganic phosphorus	p_i	$\mu\text{gP/L}$
Organic silica	s_o	mgSi/L
Inorganic silica	s_i	mgSi/L
Phytoplankton	a_{p1}	$\mu\text{gA/L}$
Herbivorous zooplankton	z_h	mgC/L
Carnivorous zooplankton	z_c	mgC/L
Phytoplankton2	a_{p2}	$\mu\text{gA/L}$
Phytoplankton3	a_{p3}	$\mu\text{gA/L}$

* $\text{mg/L} \equiv \text{g/m}^3$ and $\mu\text{g/L} \equiv \text{mg/m}^3$

A mass balance is written for each vertical layer. For the epilimnion for the case where the inflow and outflow pass directly through the epilimnion, the balance is written as

$$V_1 \frac{dc_1}{dt} = Q_{in} c_{in} - Q_{out} c_1 + E_1' (c_2 - c_1) + S_1 V_1 \quad (41)$$

where c_i = the concentration of layer i [mg/L or $\mu\text{g/L}$], c_{in} = the concentration of the inflow [mg/L or $\mu\text{g/L}$], and S_i = sources and sinks of the constituent due to reactions and mass transfer mechanisms [$\text{g/m}^3/\text{d}$ or $\text{mg/m}^3/\text{d}$]. Similar balances are written for the other layers.

The sources and sinks for the state variables are depicted in Figure 32. Note that although the model allows the simulation of three phytoplankton groups, for simplicity, the figure shows a single phytoplankton state variable. In addition, silica is omitted. The mathematical representation of these processes is presented in the following sections.

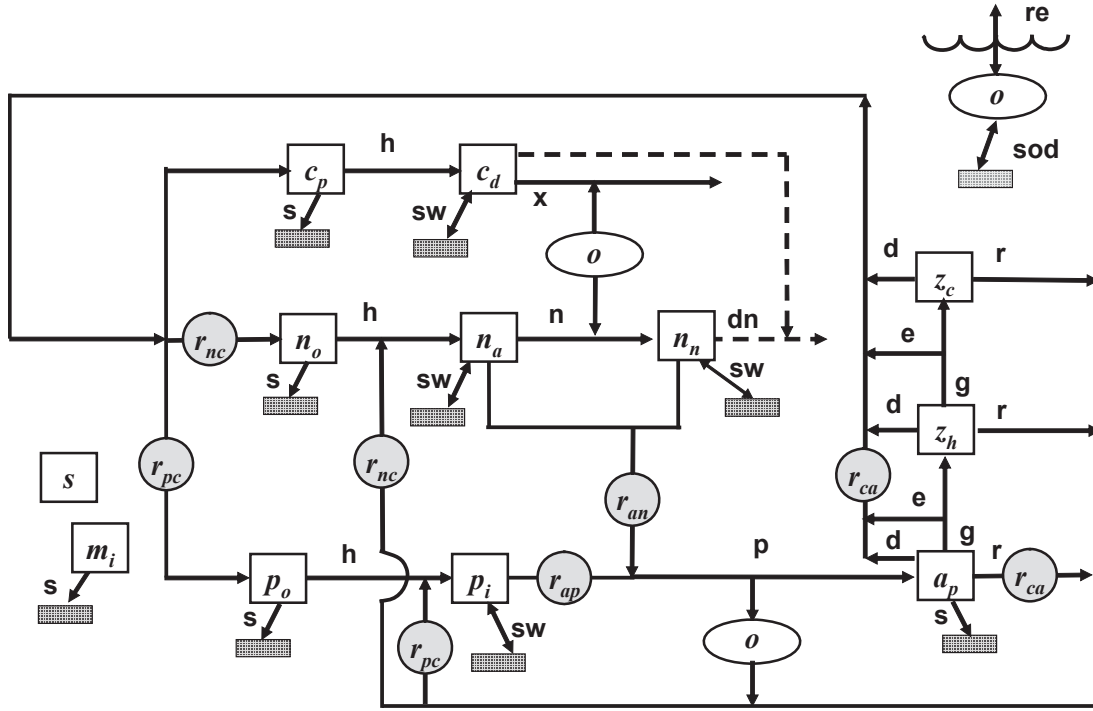


Figure 32 Model kinetics and mass transfer processes. The state variables are defined in Table 3. Kinetic processes are hydrolysis (h), oxidation (x), nitrification (n), denitrification (dn), photosynthesis (p), respiration (r), death (d), grazing (g), and egestion (e). Mass transfer processes are reaeration (re), settling (s), sediment oxygen demand (sod), and sediment-water exchange (sw).

6.2 Reaction Fundamentals

6.2.1 Biochemical Reactions

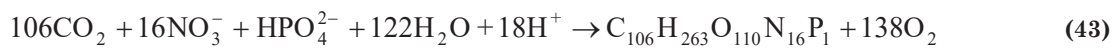
The following chemical equations are used to represent the major biochemical reactions that take place in the model (Stumm and Morgan 1996):

Plant Photosynthesis:

Ammonium as substrate:



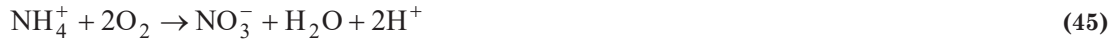
Nitrate as substrate:



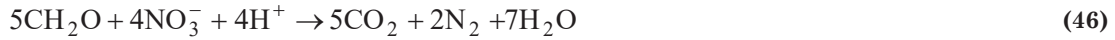
Plant Respiration:



Nitrification:



Denitrification:



6.2.2 Stoichiometry of Organic Matter

The model assumes a constant stoichiometry for organic matter (i.e., phytoplankton and zooplankton). The following representation is suggested as a first approximation (Redfield et al. 1963, Chapra 1997),

$$100 \text{ gD} : 40 \text{ gC} : 7200 \text{ mgN} : 1000 \text{ mgP} : 1000 \text{ mgA} \quad (47)$$

where gX = mass of element X [g] and mgY = mass of element Y [mg]. The terms D, C, N, P, and A refer to dry weight, carbon, nitrogen, phosphorus, and chlorophyll *a*, respectively. It should be noted that chlorophyll *a* is the most variable of these values with a range of approximately 500-2000 mgA (Laws and Chalup 1990, Chapra 1997).

These values are then combined to determine stoichiometric ratios as in

$$r_{xy} = \frac{\text{gX}}{\text{gY}} \quad (48)$$

For example, the milligrams of organic nitrogen that is released when 1 gC of carnivorous zooplankton die can be computed as

$$r_{nc} = \frac{7200 \text{ mgN}}{40 \text{ gC}} = 180 \frac{\text{mgN}}{\text{gC}}$$
$$\frac{dV}{dt} = Q_{in} + Q_p - Q_e - Q_{out} \quad (49)$$

Recommended values for stoichiometry are shown in Table 4.

Table 4 Recommended values for stoichiometry.

Dry weight	100 gD
Carbon	40 gC
Nitrogen	7.2 gN
Phosphorus	1 gP
Chlorophyll	1 gA

6.2.2.1 Oxygen Generation and Consumption

The model requires that the rates of oxygen generation and consumption be prescribed. If ammonia is the substrate, the following ratio (based on Eq. 42) can be used to determine the grams of oxygen generated for each gram of plant matter carbon that is produced through photosynthesis.

$$r_{oca} = \frac{107 \text{ moleO}_2 (32 \text{ gO}_2/\text{moleO}_2)}{106 \text{ moleC} (12 \text{ gC}/\text{moleC})} = 2.69 \frac{\text{gO}_2}{\text{gC}} \quad (50)$$

If nitrate is the substrate, the following ratio (based on Eq. 43) applies

$$r_{ocn} = \frac{138 \text{ moleO}_2 (32 \text{ gO}_2/\text{moleO}_2)}{106 \text{ moleC} (12 \text{ gC}/\text{moleC})} = 3.47 \frac{\text{gO}_2}{\text{gC}} \quad (51)$$

Note that Eq. (50) is also used to determine the amount of oxygen consumed per the amount of organic carbon produced for both plant respiration and DOC oxidation.

For nitrification, the following ratio based on Eq. (45) represents the amount of oxygen consumed per the mass of ammonia nitrogen converted to nitrate

$$r_{on} = \frac{2 \text{ moleO}_2 (32 \text{ gO}_2/\text{moleO}_2)}{1 \text{ moleN} (14 \text{ gN}/\text{moleN})} \times \frac{1 \text{ gN}}{1000 \text{ mgN}} = 0.00457 \frac{\text{gO}_2}{\text{mgN}} \quad (52)$$

6.2.2.2 DOC Utilization Due to Denitrification

Based on Eq. (46), DOC is utilized during denitrification,

$$r_{cndn} = \frac{5 \text{ moleC} \times 12 \text{ gC}/\text{moleC}}{4 \text{ moleN} \times 14 \text{ gN}/\text{moleN}} \times \frac{1 \text{ gN}}{1000 \text{ mgN}} = 0.0009375 \frac{\text{gC}}{\text{mgN}} \quad (53)$$

6.2.3 Temperature Effects on Reactions

With the exception of phytoplankton photosynthesis, the temperature effect for all first-order reactions used in the model is represented by the simplified Arrhenius or “theta” model,

$$k(T) = k(20)\theta^{T-20} \quad (54)$$

where $k(T)$ = the reaction rate [1/d] at temperature T [°C] and θ = the temperature parameter for the reaction.

6.3 Constituent Reactions

The mathematical relationships that describe the individual reactions and concentrations of the model state variables (Table 3) are presented in the following paragraphs.

6.3.1 Specific Conductance (s)

It is assumed that the specific conductance is conservative:

$$S_s = 0 \quad (55)$$

6.3.2 Phytoplankton (a_p)

Note that the model can be used to simulate three phytoplankton groups. Since all use identical formulations the following description applies to all groups. Distinctions between the groups are represented by using different parameter values.

Phytoplankton biomass increases due to photosynthesis. It is lost via respiration, death, grazing and settling

$$S_{ap} = \text{PhytoPhoto} - \text{PhytoResp} - \text{PhytoDeath} - \text{HZooGraz} - \text{PhytoSettl} \quad (56)$$

6.3.2.1 Photosynthesis

Phytoplankton photosynthesis is a function of temperature, nutrients, and light

$$\text{PhytoPhoto} = \mu_p a_p \quad (57)$$

where μ_p = phytoplankton photosynthesis rate [1/d], which is calculated as

$$\mu_p = k_{gp}(T) \phi_{Np} \phi_{Lp} \quad (58)$$

where $k_{gp}(T)$ = the maximum photosynthesis rate at temperature T [1/d], ϕ_{Np} = phytoplankton nutrient attenuation factor [dimensionless number between 0 and 1], and ϕ_{Lp} = the phytoplankton light attenuation coefficient [dimensionless number between 0 and 1].

Note that as with other model rates, the temperature dependence of phytoplankton photosynthesis can be modeled with the theta model (Eq. 54). In addition, it can also be represented by an asymmetric bell-shaped model (Cerco and Cole 1994),

$$k_{gp}(T) = k_{gp,opt} e^{-\kappa_1 (T - T_{opt})^2} \quad T \leq T_{opt} \quad (59)$$

$$k_{gp}(T) = k_{gp,opt} e^{-\kappa_2 (T - T_{opt})^2} \quad T > T_{opt} \quad (60)$$

where κ_1 and κ_2 are parameters that determine the shape of the relationship of growth to temperature below and above the optimal temperature, respectively.

Nutrient Limitation. Michaelis-Menten equations are used to represent growth limitation for inorganic nitrogen and phosphorus. The minimum value is then used to compute the nutrient attenuation factor,

$$\phi_{Np} = \min\left(\frac{n_a + n_n}{K_{sN} + n_a + n_n}, \frac{p_i}{K_{sP} + p_i}\right) \quad (61)$$

where K_{sN} = nitrogen half-saturation constant [$\mu\text{gN/L}$] and K_{sP} = phosphorus half-saturation constant [$\mu\text{gP/L}$]. Note that silica can be included if diatoms are being simulated,

$$\phi_{Np} = \min\left(\frac{n_a + n_n}{K_{sN} + n_a + n_n}, \frac{p_i}{K_{sP} + p_i}, \frac{s_i}{K_{sS} + s_i}\right)$$

where K_{sS} = silica half-saturation constant [$\mu\text{gSi/L}$] and s_i = concentration of available inorganic silica [mgSi/L].

Light Limitation. It is assumed that light attenuation through the water follows the Beer-Lambert law,

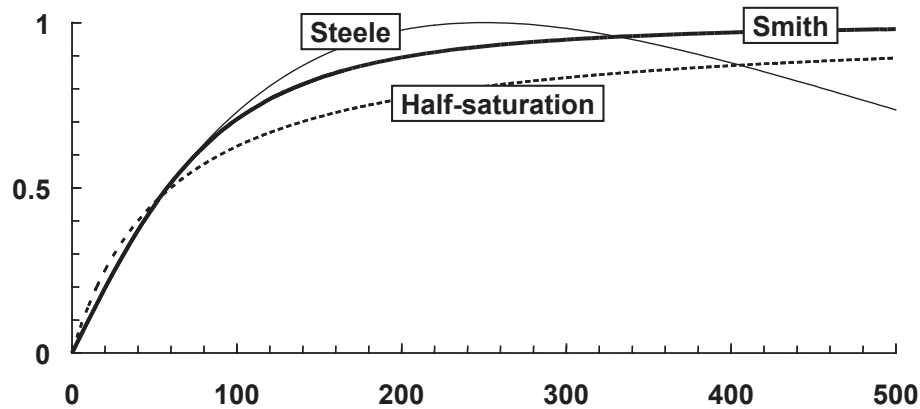
$$PAR(z) = PAR(0)e^{-K_d z} \quad (62)$$

where daytime $PAR(z)$ = the mean daytime photosynthetically available radiation (PAR) at depth z below the water surface [ly/d]¹, and K_d = the light extinction coefficient [m^{-1}]. Note that the relationship of the extinction coefficient to the model variables is discussed in Section 6.4.

The PAR at the water surface is related to the mean daily solar radiation at the water surface by (Szeicz 1984, Baker and Frouin 1987)

$$PAR(0) = \frac{0.47 I(0)}{f} \quad (63)$$

where f = the photoperiod expressed as the fraction of a day.



¹ ly/d = langley per day. A langley is equal to a calorie per square centimeter. Note that a ly/d is related to the $\mu\text{E/m}^2/\text{s}$ by the following approximation: $1 \mu\text{E/m}^2/\text{s} \cong 0.45 \text{ Langley/day}$ (LIC-OR, Lincoln, NE).

Figure 33 The three models used for phytoplankton photosynthetic light dependence. The plot shows growth attenuation versus PAR intensity [ly/d].

Three models are used to characterize the impact of light on phytoplankton photosynthesis (Figure 33):

Half-Saturation (Michaelis-Menten) Light Model (Baly 1935):

$$F_{Lp} = \frac{PAR(z)}{K_{Lp} + PAR(z)} \quad (64)$$

where F_{Lp} = phytoplankton growth attenuation due to light and K_{Lp} = the phytoplankton light parameter. In the case of the half-saturation model, the light parameter is a half-saturation coefficient [ly/d].

This function can be combined with the Beer-Lambert law and integrated over water depth to yield the phytoplankton light attenuation coefficient for layer i

$$\phi_{Lp,i} = \frac{f}{K_{d,i}H_i} \ln \left(\frac{K_{Lp} + PAR(d_i)}{K_{Lp} + PAR(d_i)e^{-K_{d,i}H_i}} \right) \quad (65)$$

where $K_{d,i}$ = the light extinction coefficient of layer i [1/m], H_i = the thickness of layer i [m], and d_i = the distance from the water surface to the top of layer i [m].

Steele's Equation (Steele 1962):

$$F_{Lp} = \frac{PAR(z)}{K_{Lp}} e^{1 - \frac{PAR(z)}{K_{Lp}}} \quad (66)$$

where K_{Lp} = the PAR at which phytoplankton growth is optimal [ly/d]. This function can be combined with the Beer-Lambert law and integrated over water depth to yield

$$\phi_{Lp,i} = \frac{2.718282f}{K_{d,i}H_i} \left(e^{-\frac{PAR(d_i)}{K_{Lp}}e^{-K_{d,i}H_i}} - e^{-\frac{PAR(d_i)}{K_{Lp}}} \right) \quad (67)$$

Smith's Function (Smith 1936):

$$F_{Lp} = \frac{PAR(z)}{\sqrt{K_{Lp}^2 + PAR(z)^2}} \quad (68)$$

where K_{Lp} = the light parameter for the Smith model [ly/d]; that is, the PAR at which growth is 70.7% of the maximum. This function can be combined with the Beer-Lambert law and integrated over water depth to yield

$$\phi_{Lp,i} = \frac{f}{K_{d,i} H_i} \ln \left(\frac{PAR(d_i) / K_{Lp} + \sqrt{1 + (PAR(d_i) / K_{Lp})^2}}{(PAR(d_i) / K_{Lp}) e^{-K_{d,i} H_i} + \sqrt{1 + ((PAR(d_i) / K_{Lp}) e^{-K_{d,i} H_i})^2}} \right) \quad (69)$$

6.3.2.2 Losses

Note that the model includes two forms of phytoplankton death: first-order death and grazing by herbivorous zooplankton. In the former, the loss of phytoplankton is represented as a simple first-order loss. This option is used when (a) herbivorous zooplankton are not explicitly simulated or (b) there are additional sources of phytoplankton mortality beyond herbivore grazing. An example would be where grazing losses by plankton-feeding fish was significant.

Respiration. Phytoplankton respiration is represented as a first-order rate,

$$\text{PhytoResp} = k_{rp}(T) a_p \quad (70)$$

where $k_{rp}(T)$ = temperature-dependent phytoplankton respiration rate [1/d].

Death. Phytoplankton death is represented as a first-order rate,

$$\text{PhytoDeath} = k_{dp}(T) a_p \quad (71)$$

where $k_{dp}(T)$ = temperature-dependent phytoplankton death rate [1/d].

Grazing. Phytoplankton are lost due to herbivorous zooplankton grazing,

$$\text{HZooGraz} = \left(C_{gh} \theta_{gh}^{T-20} \frac{F_g a_p}{k_{sa} + F_g a_p} z_h \right) F_g a_p \quad (72)$$

where C_{gh} = herbivorous zooplankton grazing rate [$\text{m}^3/(\text{gC d})$], θ_{gh} = temperature parameter for herbivorous zooplankton grazing [dimensionless], k_{sa} = chlorophyll half-saturation constant [mgA/m^3], and F_g = the grazability of the phytoplankton by the herbivorous zooplankton (dimensionless number: 0-1).

Settling. Phytoplankton settling is represented for layer i as

$$\text{PhytoSettl} = -v_a \frac{A_{i-1}}{V_i} a_{p,i-1} + v_a \frac{A_i}{V_i} a_{p,i} \quad (73)$$

where v_a = phytoplankton settling velocity [m/d], A_i = the surface area of the bottom boundary of layer i [m^2], and V_i = the volume of layer i [m^3]. Note that for all settling computations, the input from above is set to zero for the top layer.

6.3.3 Herbivorous zooplankton (z_h)

Herbivorous zooplankton increase due to grazing on phytoplankton. They are lost via respiration and carnivorous zooplankton grazing.

$$S_{zh} = r_{ca} \varepsilon_h \text{HZooGraz} - \text{HZooResp} - \text{HZooDeath} - \text{CZooGraz} \quad (74)$$

where ε_h = herbivorous zooplankton grazing efficiency [dimensionless].

6.3.3.1 Losses

Note that the model includes two forms of herbivorous zooplankton death: first-order death and grazing by carnivorous zooplankton. In the former, the loss of herbivorous zooplankton is represented as a simple first-order loss. This option is used when (a) carnivorous zooplankton are not explicitly simulated or (b) there are additional sources of herbivorous zooplankton mortality beyond carnivorous zooplankton grazing. An example would be where grazing losses by plankton-feeding fish was significant.

Respiration. Herbivorous zooplankton respiration is represented as a first-order rate,

$$\text{HZooResp} = k_{rh}(T) z_h \quad (75)$$

where $k_{rh}(T)$ = temperature-dependent herbivorous zooplankton respiration rate [/d].

Death. Herbivorous zooplankton death is represented as a first-order rate,

$$\text{HZooDeath} = k_{dh}(T) z_h \quad (76)$$

where $k_{dh}(T)$ = the temperature-dependent herbivorous zooplankton death rate [/d].

Grazing. Herbivorous zooplankton are lost due to carnivorous zooplankton grazing,

$$\text{CZooGraz} = \left(C_{gc} \theta_{gc}^{T-20} \frac{z_h}{k_{sh} + z_h} z_c \right) z_h \quad (77)$$

where C_{gc} = carnivorous zooplankton grazing rate [$\text{m}^3/(\text{gC d})$], θ_{gc} = temperature parameter for carnivorous zooplankton grazing [dimensionless], and k_{sh} = herbivore carbon half-saturation constant [gC/m^3].

6.3.4 Carnivorous zooplankton (z_c)

Carnivorous zooplankton increase due to grazing on herbivorous zooplankton. They are lost via respiration and death.

$$S_{zc} = \varepsilon_c \text{CZooGraz} - \text{CZooResp} - \text{CZooDeath} \quad (78)$$

where ε_c = carnivorous zooplankton grazing efficiency [dimensionless].

6.3.4.1 Losses

Respiration. Carnivorous zooplankton respiration is represented as a first-order rate,

$$CZooResp = k_{rc}(T) z_c \quad (79)$$

where $k_{rc}(T)$ = temperature-dependent carnivorous zooplankton respiration rate [/d].

Death. Carnivorous zooplankton death is represented as a first-order rate,

$$CZooDeath = k_{drc}(T) z_c \quad (80)$$

where $k_{drc}(T)$ = the temperature-dependent carnivorous zooplankton death rate [/d].

6.3.5 Particulate Organic Carbon (c_p)

Particulate organic carbon (POC) increases due to zooplankton egestion of phytoplankton and herbivorous zooplankton, and death of phytoplankton, herbivorous zooplankton, and carnivorous zooplankton. It is lost via hydrolysis and settling.

$$S_{cs} = r_{ca}(1 - \varepsilon_h)HZooGraz + (1 - \varepsilon_c)CZooGraz + a_{ca}PhytoDeath \\ HZooDeath + CZooDeath - POCHydr - POCSettl \quad (81)$$

where

$$POCHydr = k_{hc}(T)c_p \quad (82)$$

where $k_{hc}(T)$ = the temperature-dependent POC hydrolysis rate [/d].

POC settling is represented for layer i by

$$POCSettl = -v_{oc} \frac{A_{i-1}}{V_i} c_{p,i-1} + v_{oc} \frac{A_i}{V_i} c_{p,i} \quad (83)$$

where v_{oc} = POC settling velocity [m/d].

6.3.6 Dissolved Organic Carbon (c_d)

Fast reacting CBOD is gained via the hydrolysis of slowly-reacting CBOD. It is lost via oxidation and denitrification.

$$S_{cf} = POCHydr - DOCOxid - r_{cndn} Denitr \quad (84)$$

where

$$DOCOxid = F_{oxcd} k_{dc}(T)c_d \quad (85)$$

where $k_{dc}(T)$ = the temperature-dependent DOC oxidation rate [/d] and F_{oxcd} = attenuation due to low oxygen [dimensionless]. The parameter r_{cndn} is the ratio of organic carbon lost per nitrate nitrogen that is denitrified (Eq. 49). The term Denitr is the rate of denitrification [$\mu\text{gN/L/d}$]. It will be defined in Section 6.3.9 below.

Two formulations are used to represent the oxygen attenuation of the oxidation rate:

Saturating Exponential:

$$F_{oxcd} = (1 - e^{-K_{sacd}o}) \quad (86)$$

where K_{sacd} = exponential coefficient for the effect of oxygen on DOC oxidation [L/mgO_2].

Half-Saturation:

$$F_{oxcd} = \frac{o}{K_{sacd} + o} \quad (87)$$

where K_{sacd} = half-saturation constant for the effect of oxygen on DOC oxidation [mgO_2/L].

6.3.7 Organic Nitrogen (n_o)

Organic nitrogen increases due to zooplankton egestion of phytoplankton and herbivorous zooplankton, and death of phytoplankton, herbivorous zooplankton, and carnivorous zooplankton. It is lost via hydrolysis and settling.

$$\begin{aligned} S_{no} = & r_{na}(1 - \varepsilon_h)\text{HZooGraz} + r_{nc}(1 - \varepsilon_c)\text{CZooGraz} + r_{na}\text{PhytoDeath} \\ & + r_{nc}\text{HZooDeath} + r_{nc}\text{CZooDeath} - \text{NorgHydr} - \text{NorgSettl} \end{aligned} \quad (88)$$

where

$$\text{NorgHydr} = k_{hn}(T)n_o \quad (89)$$

where $k_{hn}(T)$ = the temperature-dependent organic nitrogen hydrolysis rate [/d].

Organic N settling is represented for layer i by

$$\text{NorgSettl} = -v_{on} \frac{A_{i-1}}{V_i} n_{o,i-1} + v_{on} \frac{A_i}{V_i} n_{o,i} \quad (90)$$

where v_{on} = organic nitrogen settling velocity [m/d].

6.3.8 Ammonia Nitrogen (n_a)

Ammonia nitrogen increases due to organic nitrogen hydrolysis and respiration. It is lost via nitrification and plant photosynthesis:

$$S_{na} = \text{NorgHydr} + r_{na} \text{PhytoResp} + r_{nc} \text{HZooResp} + r_{nc} \text{CZooResp} - \text{NH4Nitrif} - r_{na} P_{ap} \text{PhytoPhoto} \quad (91)$$

The ammonia nitrification rate is computed as

$$\text{NH4Nitrif} = F_{oxna} k_n(T) n_a \quad (92)$$

where $k_n(T)$ = the temperature-dependent nitrification rate for ammonia nitrogen [1/d] and F_{oxna} = attenuation due to low oxygen [dimensionless]. Oxygen attenuation is modeled by Eqs. (86) and (87) with the oxygen dependency represented by the parameter K_{sona} .

The coefficient P_{ap} is the phytoplankton preference for ammonium as a nitrogen source,

$$P_{ap} = \frac{n_a n_n}{(k_{hnxp} + n_a)(k_{hnxp} + n_n)} + \frac{n_a k_{hnxp}}{(n_a + n_n)(k_{hnxp} + n_n)} \quad (93)$$

where k_{hnxp} = preference coefficient of phytoplankton for ammonium [mgN/m³].

6.3.9 Nitrate Nitrogen (n_n)

Nitrate nitrogen increases due to nitrification of ammonia. It is lost via denitrification and plant photosynthesis:

$$S_{ni} = \text{NH4Nitrif} - \text{Denitr} - r_{na} (1 - P_{ap}) \text{PhytoPhoto} \quad (94)$$

The denitrification rate is computed as

$$\text{Denitr} = (1 - F_{oxdn}) \frac{c_d}{K_{sdoc} + c_d} k_{dn}(T) n_n \quad (95)$$

where $k_{dn}(T)$ = the temperature-dependent denitrification rate of nitrate nitrogen [1/d], K_{sdoc} = DOC half-saturation constant for denitrification [gC/m³], F_{oxdn} = effect of low oxygen on denitrification [dimensionless] as modeled by Eqs. (86) and (87) with the oxygen dependency represented by the parameter K_{sodn} .

6.3.10 Organic Phosphorus (p_o)

Organic phosphorus increases due to zooplankton egestion of phytoplankton and herbivorous zooplankton, and death of phytoplankton, herbivorous zooplankton, and carnivorous zooplankton. It is lost via hydrolysis and settling.

$$S_{po} = r_{pa}(1 - \varepsilon_h) \text{HZooGraz} + r_{pc}(1 - \varepsilon_c) \text{CZooGraz} + r_{pa} \text{PhytoDeath} + r_{pc} \text{HZooDeath} + r_{pc} \text{CZooDeath} - \text{PorgHydr} - \text{PorgSettl} \quad (96)$$

where

$$\text{PorgHydr} = k_{hp}(T) p_o \quad (97)$$

where $k_{hp}(T)$ = the temperature-dependent organic phosphorus hydrolysis rate [/d].

Organic P settling is represented for layer i by

$$\text{PorgSettl} = -v_{op} \frac{A_{i-1}}{V_i} p_{o,i-1} + v_{op} \frac{A_i}{V_i} p_{o,i} \quad (98)$$

where v_{op} = organic phosphorus settling velocity [m/d].

6.3.11 Inorganic Phosphorus (p_i)

Inorganic phosphorus increases due to organic phosphorus hydrolysis and respiration. It is lost via plant photosynthesis:

$$S_{pi} = \text{PorgHydr} + r_{pa} \text{PhytoResp} + r_{pc} \text{HZooResp} + r_{pc} \text{CZooResp} - r_{pa} \text{PhytoPhoto} \quad (99)$$

6.3.12 Inorganic Suspended Solids (m_i)

Inorganic suspended solids are lost via settling,

$$S_{mi} = -\text{InorgSettl}$$

where for layer j ,

$$\text{InorgSettl} = -v_i \frac{A_{j-1}}{V_j} m_{i,j-1} + v_i \frac{A_j}{V_j} m_{i,j} \quad (100)$$

where v_i = inorganic suspended solids settling velocity [m/d].

6.3.13 Dissolved Oxygen (o)

Dissolved oxygen increases due to plant photosynthesis. It is lost via DOC oxidation, nitrification and respiration. Depending on whether the water is undersaturated or oversaturated it is gained or lost via reaeration,

$$S_o = r_{ca} (r_{oca} P_{ap} + r_{ocn} (1 - P_{ap})) \text{PhytoPhoto} - r_{oca} \text{FastCOxid} - r_{on} \text{NH4Nitr} - r_{ca} r_{oca} \text{PhytoResp} - r_{oca} \text{HZooResp} - r_{oca} \text{CZooResp} + \text{OxReaer} \quad (101)$$

where

$$\text{OxReaer} = \frac{K_L A_0}{V_1} (o_s(T_1, elev) - o) \quad (102)$$

where K_L = the oxygen mass-transfer coefficient [m/d], $o_s(T_1, elev)$ = the saturation concentration of oxygen [mgO₂/L] at the temperature of the surface layer, T_1 [°C], and elevation above sea level of the lake's surface, $elev$.

The following equation is used to represent the dependence of oxygen saturation on temperature (APHA 1995)

$$\ln o_s(T_1, 0) = -139.34411 + \frac{1.575701 \times 10^5}{T_a} - \frac{6.642308 \times 10^7}{T_a^2} + \frac{1.243800 \times 10^{10}}{T_a^3} - \frac{8.621949 \times 10^{11}}{T_a^4} \quad (103)$$

where $o_s(T_1, 0)$ = the saturation concentration of dissolved oxygen in freshwater at 1 atm [mgO₂/L] and T_a = absolute temperature [K] where $T_a = T_1 + 273.15$.

The effect of atmospheric pressure on gas saturation at elevation is based on the standard atmosphere as described by the cubic polynomial (Camacho and Chapra 2020):

$$\phi_{elev} = 1 - 0.11988 elev + 6.10834 \times 10^{-3} elev^2 - 1.60747 \times 10^{-4} elev^3 \quad (104)$$

where $elev$ = the elevation above sea level of the lake's surface [km]. Note that the software has elevation in meters and then internally changes it to km.

6.3.13.1 Reaeration Formulas

Three methods are used to represent the dependence of oxygen gas transfer on temperature and wind speed. Two consist of simple formulas, whereas the third consists of a more elaborate algorithm.

Banks-Herrera formula (Banks 1975, Banks and Herrera 1977):

$$K_l = (0.728U_w^{0.5} - 0.317U_w + 0.0372U_w^2) \theta_{ka}^{T-20} \quad (105)$$

Wanninkhof formula (Wanninkhof 1991):

$$K_l = (0.0986U_w^{1.64}) \theta_{ka}^{T-20} \quad (106)$$

where K_l = the oxygen mass-transfer coefficient [m d⁻¹], U_w = wind speed measured 10 meters above the water surface [m s⁻¹] and θ_{ka} = the temperature parameter for oxygen gas transfer

[suggested value: 1.024]. Note that the model uses Eq. (34) to correct the wind velocity (7 meters above the surface) entered on the Meteorology worksheet (Figure 13) so that it is scaled to the 10-m height.

O'Connor Algorithm (O'Connor 1983):

O'Connor (1983) has developed a theoretically based set of formulas to compute gas transfer for low-solubility gases such as oxygen. Appendix B describes how the O'Connor algorithm is computed.

6.4 LIGHT MODEL AND SECCHI DEPTH

The extinction coefficient is related to model variables by (Di Toro 1978)

$$K_d = a + (1 - \gamma)b \quad (107)$$

where a = the absorption coefficient [m^{-1}], γ = the fraction of particle scattering that is directly forward scattered [dimensionless], and b = the scattering coefficient [m^{-1}].

The absorption coefficient is related to the model variables by

$$a = a_w + a_c + \alpha_{chl}a_p + \alpha_{POC}r_{dc}c_p + \alpha_i m_i \quad (108)$$

where a_w = the absorption coefficient due to water [m^{-1}], a_c = the absorption coefficient due to color [m^{-1}], α_{chl} = absorption proportionality constant for chlorophyll a [m^2/mgA], α_{POC} = absorption proportionality constant for POC expressed as dry weight [m^2/gD], and α_i = absorption proportionality constant for inorganic solids [m^2/gD].

The scattering coefficient is related to the model variables by

$$b = b_w + \beta_{chl}a_p + \beta_{POC}r_{dc}c_p + \beta_i m_i \quad (109)$$

where b_w = the scattering coefficient due to water [m^{-1}], β_{chl} = scattering proportionality constant for chlorophyll a [m^2/mgA], β_{POC} = scattering proportionality constant for POC expressed as dry weight [m^2/gD], and β_i = scattering proportionality constant for inorganic solids [m^2/gD]. Recommended values for the light-related coefficients are listed in Table 5.

Table 5 Suggested values for light extinction coefficients

Symbol	Value	Reference
γ	0.94	Di Toro (1978)
a_w	0.012	Kirk (1994)
a_c	system specific	
α_{chl}	0.030	Di Toro (1978)
α_{POC}	0.16	Di Toro (1978)
α_i	0.031	Di Toro (1978)

b_w	0.0027	Kirk (1994)
β_{chl}	0.010	Di Toro (1978)
β_{POC}	0.24	Di Toro (1978)
β_i	0.37	Di Toro (1978)

The Secchi depth, SD [m], is calculated with (Tyler 1968, Preisendorfer 1986),

$$SD = \frac{8.7}{K_d + c} \quad (110)$$

where c = beam attenuation coefficient [m^{-1}], which is equal to the sum of the absorption and scattering coefficients,

$$c = a + b \quad (111)$$

6.5 SOD/Nutrient Flux Model

Sediment nutrient fluxes and sediment oxygen demand (SOD) are based on a model originally developed by Di Toro (Di Toro et al. 1991, Di Toro and Fitzpatrick. 1993, Di Toro 2001).

A schematic of the model is depicted in Figure 34. As can be seen, the approach allows oxygen and nutrient sediment-water fluxes to be computed based on the downward flux of particulate organic matter from the overlying water. The sediments are divided into 2 layers: a thin ($\cong 1$ mm) surface aerobic layer underlain by a thicker (10 cm) lower anaerobic layer. Organic carbon, nitrogen and phosphorus are delivered to the anaerobic sediments via the settling of particulate organic matter (i.e., phytoplankton and detritus). There they are transformed by mineralization reactions into dissolved methane, ammonium and inorganic phosphorus. These constituents are then transported to the aerobic layer where some of the methane and ammonium are oxidized. The flux of oxygen from the water required for these oxidations is the sediment oxygen demand. The following sections provide details on how the model computes this SOD along with the sediment-water fluxes of carbon, nitrogen and phosphorus that are also generated in the process.

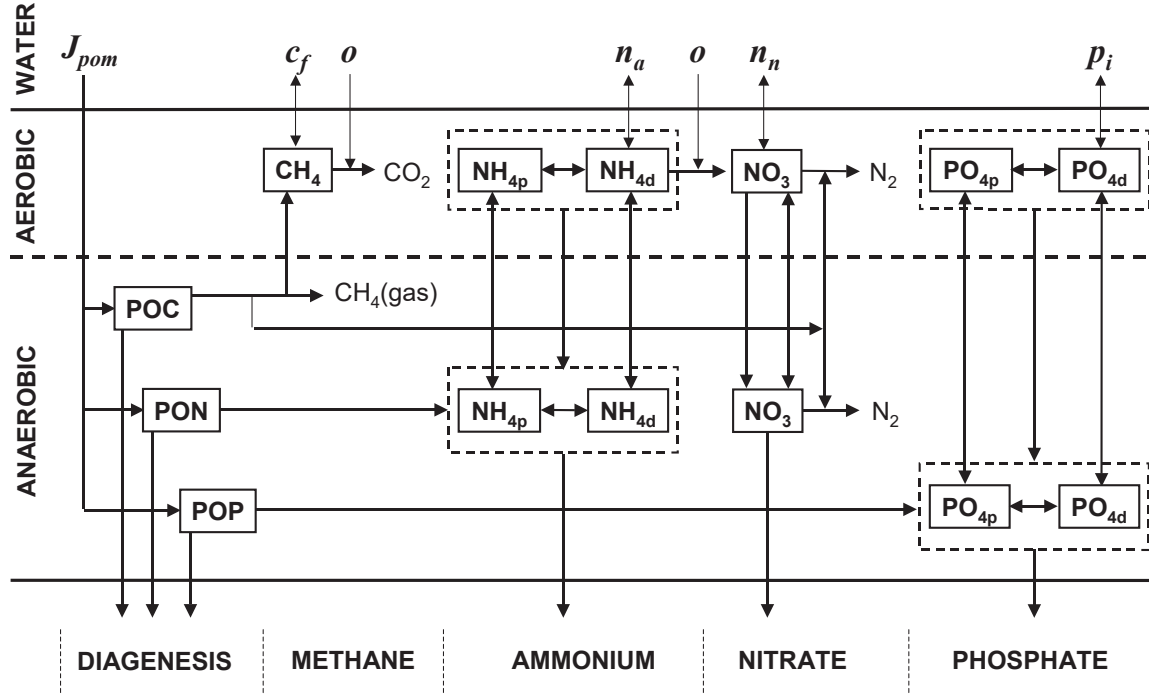


Figure 34 Schematic of SOD-nutrient flux model of the sediments.

6.5.1 Diagenesis

As summarized in Figure 35, the first step in the computation involves determining how much of the downward flux of particulate organic matter (POM) is converted into soluble reactive forms in the anaerobic sediments. This process is referred to as diagenesis. First the total downward flux is computed as the sum of the fluxes of phytoplankton and detritus settling from the water column

$$J_{POM} = r_{da} v_a a_p + v_{dt} m_o \quad (112)$$

where J_{POM} = the downward flux of POM [$\text{gD m}^{-2} \text{d}^{-1}$], r_{da} = the ratio of dry weight to chlorophyll a [gD/mgA], v_a = phytoplankton settling velocity [m/d], a_p = phytoplankton concentration [mgA/m^3], v_{dt} = detritus settling velocity [m/d], and m_o = detritus concentration [gD/m^3].

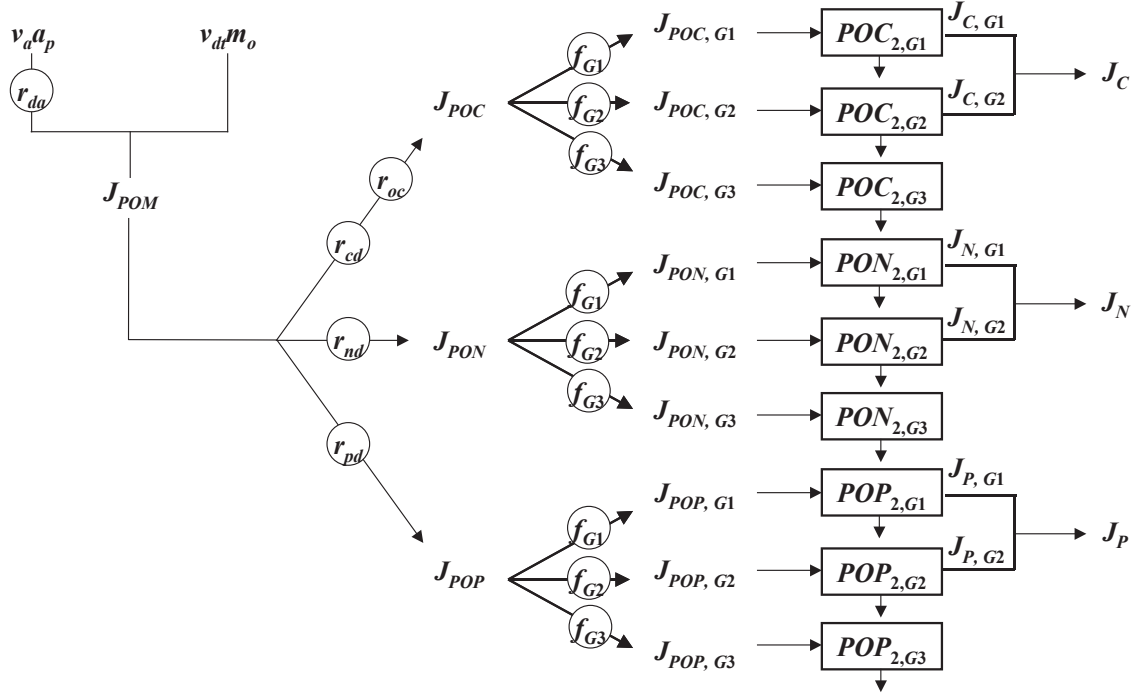


Figure 35 Representation of how settling particulate organic particles (phytoplankton and detritus) are transformed into fluxes of dissolved carbon (J_C), nitrogen (J_N) and phosphorus (J_P) in the anaerobic sediments.

Stoichiometric ratios are then used to divide the POM flux into carbon, nitrogen and phosphorus. Note that for convenience, we will express the particulate organic carbon (POC) as oxygen equivalents using the stoichiometric coefficient r_{oc} . Each of the nutrient fluxes is further broken down into three reactive fractions: labile (G1), slowly reacting (G2) and non-reacting (G3).

These fluxes are then entered into mass balances to compute the concentration of each fraction in the anaerobic layer. For example, for labile POC, a mass balance is written as

$$H_2 \frac{dPOC_{2,G1}}{dt} = J_{POC,G1} - k_{POC,G1} \theta_{POC,G1}^{T-20} H_2 POC_{2,G1} - w_2 POC_{2,G1} \quad (113)$$

where H_2 = the thickness of the anaerobic layer [m], $POC_{2,G1}$ = the concentration of the labile fraction of POC in the anaerobic layer [gO_2/m^3], $J_{POC,G1}$ = the flux of labile POC delivered to the anaerobic layer [$\text{gO}_2/\text{m}^2/\text{d}$], $k_{POC,G1}$ = the mineralization rate of labile POC [d^{-1}], $\theta_{POC,G1}$ = temperature parameter for labile POC mineralization [dimensionless], and w_2 = the burial velocity [m/d]. At steady state, Eq. (113) can be solved for

$$POC_{2,G1} = \frac{J_{POC,G1}}{k_{POC,G1} \theta_{POC,G1}^{T-20} H_2 + v_b} \quad (114)$$

The flux of labile dissolved carbon, $J_{C,G1}$ [$\text{gO}_2/\text{m}^2/\text{d}$], can then be computed as

$$J_{C,G1} = k_{POC,G1} \theta_{POC,G1}^{T-20} H_2 POC_{2,G1} \quad (115)$$

In a similar fashion, a mass balance can be written and solved for the slowly reacting dissolved organic carbon (G2). This result is then added to Eq. (115) to arrive at the total flux of dissolved carbon generated in the anaerobic sediments.

$$J_C = J_{C,G1} + J_{C,G2} \quad (116)$$

Similar equations are developed to compute the diagenesis fluxes of nitrogen, J_N [gN/m²/d], and phosphorus J_P [gP/m²/d].

6.5.2 Ammonium

Based on the mechanisms depicted in Figure 34, mass balances can be written for total ammonium in the aerobic layer and the anaerobic layers,

$$\begin{aligned} H_1 \frac{dNH_{4,1}}{dt} = & \omega_{12} (f_{pa2} NH_{4,2} - f_{pa1} NH_{4,1}) + K_{L12} (f_{da2} NH_{4,2} - f_{da1} NH_{4,1}) - w_2 NH_{4,1} \\ & + s \left(\frac{n_a}{1000} - f_{da1} NH_{4,1} \right) - \frac{\kappa_{NH4,1}^2}{s} \theta_{NH4}^{T-20} \frac{K_{NH4}}{K_{NH4} + NH_{4,1}} \frac{o}{2K_{NH4,O2} + o} f_{da1} NH_{4,1} \end{aligned} \quad (117)$$

$$\begin{aligned} H_2 \frac{dNH_{4,2}}{dt} = & J_N + \omega_{12} (f_{pa1} NH_{4,1} - f_{pa2} NH_{4,2}) + K_{L12} (f_{da1} NH_{4,1} - f_{da2} NH_{4,2}) \\ & + w_2 (NH_{4,1} - NH_{4,2}) \end{aligned} \quad (118)$$

where H_1 = the thickness of the aerobic layer [m], $NH_{4,1}$ and $NH_{4,2}$ = the concentration of total ammonium in the aerobic layer and the anaerobic layers, respectively [gN/m³], n_a = the ammonium concentration in the overlying water [mgN/m³], $\kappa_{NH4,1}$ = the reaction velocity for nitrification in the aerobic sediments [m/d], θ_{NH4} = temperature parameter for nitrification [dimensionless], K_{NH4} = ammonium half-saturation constant [gN/m³], o = the dissolved oxygen concentration in the overlying water [gO₂/m³], and $K_{NH4,O2}$ = oxygen half-saturation constant [mgO₂/L], and J_N = the diagenesis flux of ammonium [gN/m²/d].

The fraction of ammonium in dissolved (f_{dai}) and particulate (f_{pai}) form are computed as

$$f_{dai} = \frac{1}{1 + m_i \pi_{ai}} \quad (119)$$

$$f_{pai} = 1 - f_{dai} \quad (120)$$

where m_i = the solids concentration in layer i [gD/m³], and π_{ai} = the partition coefficient for ammonium in layer i [m³/gD].

The mass transfer coefficient for particle mixing due to bioturbation between the layers, ω_{12} [m/d], is computed as

$$\omega_{12} = \frac{D_p \theta_{Dp}^{T-20}}{H_2} \frac{POC_{2,G1} / r_{oc}}{POC_R} \frac{o}{K_{M,Dp} + o} \quad (121)$$

where D_p = diffusion coefficient for bioturbation [m²/d], θ_{Dp} = temperature coefficient [dimensionless], POC_R = reference G1 concentration for bioturbation [gC/m³] and $K_{M,Dp}$ = oxygen half-saturation constant for bioturbation [gO₂/m³].

The mass transfer coefficient for pore water diffusion between the layers, K_{L12} [m/d], is computed as,

$$K_{L12} = \frac{D_d \theta_{Dd}^{T-20}}{H_2 / 2} \quad (122)$$

where D_d = pore water diffusion coefficient [m²/d], and θ_{Dd} = temperature coefficient [dimensionless].

The mass transfer coefficient between the water and the aerobic sediments, s [m/d], is computed as

$$s = \frac{SOD}{o} \quad (123)$$

where SOD = the sediment oxygen demand [gO₂/m²/d].

At steady state, Eqs. (117) and (118) are two simultaneous nonlinear algebraic equations. The equations can be linearized by assuming that the $NH_{4,1}$ term in the Monod term for nitrification is constant. The simultaneous linear equations can then be solved for $NH_{4,1}$ and $NH_{4,2}$. The flux of ammonium to the overlying water can then be computed as

$$J_{NH4} = s \left(f_{da1} NH_{4,1} - \frac{n_a}{1000} \right) \quad (124)$$

6.5.3 Nitrate

Mass balances for nitrate can be written for the aerobic and anaerobic layers as

$$H_1 \frac{dNO_{3,1}}{dt} = K_{L12} (NO_{3,2} - NO_{3,1}) - w_2 NO_{3,1} + s \left(\frac{n_n}{1000} - NO_{3,1} \right) + \frac{\kappa_{NH4,1}^2}{s} \theta_{NH4}^{T-20} \frac{K_{NH4}}{K_{NH4} + NH_{4,1}} \frac{o}{2K_{NH4,O2} + o} f_{da1} NH_{4,1} - \frac{\kappa_{NO3,1}^2}{s} \theta_{NO3}^{T-20} NO_{3,1} \quad (125)$$

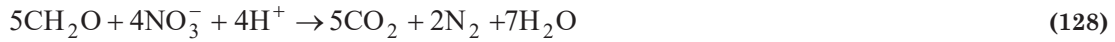
$$H_2 \frac{dNO_{3,2}}{dt} = J_N + K_{L12} (NO_{3,1} - NO_{3,2}) + w_2 (NO_{3,1} - NO_{3,2}) - \kappa_{NO3,2} \theta_{NO3}^{T-20} NO_{3,2} \quad (126)$$

where $NO_{3,1}$ and $NO_{3,2}$ = the concentration of nitrate in the aerobic layer and the anaerobic layers, respectively [gN/m^3], n_n = the nitrate concentration in the overlying water [mgN/m^3], $\kappa_{NO3,1}$ and $\kappa_{NO3,2}$ = the reaction velocities for denitrification in the aerobic and anaerobic sediments, respectively [m/d], and θ_{NO3} = temperature parameter for denitrification [dimensionless].

In the same fashion as for Eqs. (117) and (118), Eqs. (125) and (126) can be linearized and solved for $NO_{3,1}$ and $NO_{3,2}$. The flux of nitrate to the overlying water can then be computed as

$$J_{NO3} = s \left(NO_{3,1} - \frac{n_n}{1000} \right) \quad (127)$$

Denitrification requires a carbon source as represented by the following chemical equation,



The carbon requirement (expressed in oxygen equivalents per nitrogen) can therefore be computed as

$$r_{ondn} = 2.67 \frac{gO_2}{gC} \frac{5 \text{ moleC} \times 12 \text{ gC/moleC}}{4 \text{ moleN} \times 14 \text{ gN/moleN}} \times \frac{1 \text{ gN}}{1000 \text{ mgN}} = 0.00286 \frac{gO_2}{mgN} \quad (129)$$

Therefore, the oxygen equivalents consumed during denitrification, $J_{O2,dn}$ [$gO_2/m^2/d$], can be computed as

$$J_{O2,dn} = 1000 \frac{mgN}{gN} \times r_{ondn} \left(\frac{\kappa_{NO3,1}^2}{s} \theta_{NO3}^{T-20} NO_{3,1} + \kappa_{NO3,2} \theta_{NO3}^{T-20} NO_{3,2} \right) \quad (130)$$

6.5.4 Methane

The dissolved carbon generated by diagenesis is converted to methane in the anaerobic sediments. Because methane is relatively insoluble, its saturation can be exceeded and methane gas produced. As a consequence, rather than write a mass balance for methane in the anaerobic layer, an analytical model developed by Di Toro et al. (1990) is used to determine the steady-state flux of dissolved methane corrected for gas loss delivered to the aerobic sediments.

First, the carbon diagenesis flux is corrected for the oxygen equivalents consumed during denitrification,

$$J_{CH4,T} = J_C - J_{O2,dn} \quad (131)$$

where $J_{CH4,T}$ = the carbon diagenesis flux corrected for denitrification [$gO_2/m^2/d$]. In other words, this is the total anaerobic methane production flux expressed in oxygen equivalents.

If $J_{CH4,T}$ is sufficiently large ($\geq 2K_{L12}C_s$), methane gas will form. In such cases, the flux can be corrected for the gas loss,

$$J_{CH_4,d} = \sqrt{2K_{L12}C_s J_{CH_4,T}} \quad (132)$$

where $J_{CH_4,d}$ = the flux of dissolved methane (expressed in oxygen equivalents) that is generated in the anaerobic sediments and delivered to the aerobic sediments [$\text{gO}_2/\text{m}^2/\text{d}$], C_s = the saturation concentration of methane expressed in oxygen equivalents [mgO_2/L]. If $J_{CH_4,T} < 2K_{L12}C_s$, then no gas forms and

$$J_{CH_4,d} = J_{CH_4,T} \quad (133)$$

The methane saturation concentration is computed as

$$C_s = 100 \left(1 + \frac{H}{10} \right) 1.024^{20-T} \quad (134)$$

where H = water depth [m] and T = water temperature [$^{\circ}\text{C}$].

A methane mass balance can then be written for the aerobic layer as

$$H_1 \frac{dCH_{4,1}}{dt} = J_{CH_4,d} + s(c_f - CH_{4,1}) - \frac{\kappa_{CH_4,1}^2}{s} \theta_{CH_4}^{T-20} CH_{4,1} \quad (135)$$

where $CH_{4,1}$ = methane concentration in the aerobic layer [gO_2/m^3], c_f = DOC in the overlying water [gO_2/m^3], $\kappa_{CH_4,1}$ = the reaction velocity for methane oxidation in the aerobic sediments [m/d], and θ_{CH_4} = temperature parameter [dimensionless]. At steady, state, this balance can be solved for

$$CH_{4,1} = \frac{J_{CH_4,d} + s c_f}{s + \frac{\kappa_{CH_4,1}^2}{s} \theta_{CH_4}^{T-20}} \quad (136)$$

The flux of methane to the overlying water, J_{CH_4} [$\text{gO}_2/\text{m}^2/\text{d}$], can then be computed as

$$J_{CH_4} = s(CH_{4,1} - c_f) \quad (137)$$

6.5.5 SOD

The SOD [$\text{gO}_2/\text{m}^2/\text{d}$] is equal to the sum of the oxygen consumed in methane oxidation and nitrification,

$$SOD = CSOD + NSOD \quad (138)$$

where $CSOD$ = the amount of oxygen demand generated by methane oxidation [$\text{gO}_2/\text{m}^2/\text{d}$] and $NSOD$ = the amount of oxygen demand generated by nitrification [$\text{gO}_2/\text{m}^2/\text{d}$]. These are computed as

$$CSOD = \frac{\kappa_{CH4,1}^2}{S} \theta_{CH4}^{T-20} CH_{4,1} \quad (139)$$

$$NSOD = r_{on} \frac{\kappa_{NH4,1}^2}{S} \theta_{NH4}^{T-20} \frac{K_{NH4}}{K_{NH4} + NH_{4,1}} \frac{o}{2K_{NH4,O2} + o} f_{da1} NH_{4,1} \quad (140)$$

where r_{on} = the ratio of oxygen to nitrogen consumed during nitrification [= 4.57 gO₂/gN].

6.5.6 Inorganic Phosphorus

Mass balances can be written total inorganic phosphorus in the aerobic layer and the anaerobic layers as

$$H_1 \frac{dPO_{4,1}}{dt} = \omega_{12} (f_{pp2} PO_{4,2} - f_{pp1} PO_{4,1}) + K_{L12} (f_{dp2} PO_{4,2} - f_{dp1} PO_{4,1}) - w_2 PO_{4,1} + s \left(\frac{p_i}{1000} - f_{da1} PO_{4,1} \right) \quad (141)$$

$$H_2 \frac{dPO_{4,2}}{dt} = J_P + \omega_{12} (f_{pp1} PO_{4,1} - f_{pp2} PO_{4,2}) + K_{L12} (f_{dp1} PO_{4,1} - f_{dp2} PO_{4,2}) + w_2 (PO_{4,1} - PO_{4,2}) \quad (142)$$

where $PO_{4,1}$ and $PO_{4,2}$ = the concentration of total inorganic phosphorus in the aerobic layer and the anaerobic layers, respectively [gP/m³], p_i = the inorganic phosphorus in the overlying water [mgP/m³], and J_P = the diagenesis flux of phosphorus [gP/m²/d].

The fraction of phosphorus in dissolved (f_{dpi}) and particulate (f_{ppi}) form are computed as

$$f_{dpi} = \frac{1}{1 + m_i \pi_{pi}} \quad (143)$$

$$f_{ppi} = 1 - f_{dpi} \quad (144)$$

where π_{pi} = the partition coefficient for inorganic phosphorus in layer i [m³/gD].

The partition coefficient in the anaerobic layer is set to an input value. For the aerobic layer, if the oxygen concentration in the overlying water column exceeds a critical concentration, O_{crit} [gO₂/m³], then the partition coefficient is increased to represent the sorption of phosphorus onto iron oxyhydroxides as in

$$\pi_{p1} = \pi_{p2} (\Delta \pi_{PO4,1}) \quad (145)$$

where $\Delta \pi_{PO4,1}$ is a factor that increases the aerobic layer partition coefficient relative to the anaerobic coefficient.

If the oxygen concentration falls below o_{crit} then the partition coefficient is decreased smoothly until it reaches the anaerobic value at zero oxygen,

$$\pi_{p1} = \pi_{p2} \left(\Delta \pi_{PO4,1} \right)^{o/o_{crit}} \quad (146)$$

Equations (141) and (142) can be solved for $PO_{4,1}$ and $PO_{4,2}$. The flux of phosphorus to the overlying water can then be computed as

$$J_{PO4} = s \left(PO_{4,1} - \frac{p_i}{1000} \right) \quad (147)$$

6.5.7 Solution Scheme

Although the foregoing sequence of equations can be solved, a single computation will not yield a correct result because of the interdependence of the equations. For example, the surface mass transfer coefficient s depends on SOD. The SOD in turn depends on the ammonium and methane concentrations which themselves are computed via mass balances that depend on s . Hence, an iterative technique must be used. The procedure used in LAKE2K is

1. Determine the diagenesis fluxes: J_C , J_N and J_P .
2. Start with an initial estimate of SOD,

$$SOD_{init} = J_C + r_{on}' J_N \quad (148)$$

where r_{on}' = the ratio of oxygen to nitrogen consumed for total conversion of ammonium to nitrogen gas via nitrification/denitrification [= 1.714 gO₂/gN]. This ratio accounts for the carbon utilized for denitrification.

3. Compute s using

$$s = \frac{SOD_{init}}{o} \quad (149)$$

4. Solve for ammonium, nitrate and methane, and compute the $CSOD$ and $NSOD$.
5. Make a revised estimate of SOD using the following weighted average

$$SOD = \frac{SOD_{init} + CSOD + NSOD}{2} \quad (150)$$

6. Check convergence by calculating an approximate relative error

$$\varepsilon_a = \left| \frac{SOD - SOD_{init}}{SOD} \right| \times 100\% \quad (151)$$

7. If ε_a is greater than a prespecified stopping criterion ε_s then set $SOD_{init} = SOD$ and return to step 2.
8. If convergence is adequate ($\varepsilon_a \leq \varepsilon_s$), then compute the inorganic phosphorus concentrations.
9. Compute the ammonium, nitrate, methane and phosphate fluxes.

6.5.8 Supplementary Fluxes

Because of the presence of organic matter deposited prior to the summer steady-state period (e.g., during spring runoff), it is possible that the downward flux of particulate organic matter is insufficient to generate the observed SOD. In such cases, a supplementary SOD can be prescribed,

$$SOD_t = SOD + SOD_s \quad (152)$$

where SOD_t = the total sediment oxygen demand [$\text{gO}_2/\text{m}^2/\text{d}$], and SOD_s = the supplementary SOD [$\text{gO}_2/\text{m}^2/\text{d}$]. In addition, prescribed ammonia and methane fluxes can be used to supplement the computed fluxes.

7 APPENDIX A: DENSITY OF WATER

The density of water is related to temperature and salinity by (Millero and Poisson 1981):

$$\rho = \rho_o + AS + BS^{3/2} + CS^2$$

where ρ = density [g L^{-1}], S = salinity (ppt), and

$$a = 0.824493 - 0.0040899T + 0.000076438T^2 - 0.00000082467T^3 + 0.0000000053875T^4$$

$$b = -0.00572466 + 0.00010227T - 0.0000016546T^2$$

$$c = 0.00048314$$

in which T = temperature ($^{\circ}\text{C}$) and ρ_o = the density of fresh water [g L^{-1}],

$$\begin{aligned} \rho_o = & 999.842594 + 0.06793952T - 9.095290 \times 10^{-3}T^2 + 1.001685 \times 10^{-4}T^3 \\ & - 1.120083 \times 10^{-6}T^4 + 6.536332 \times 10^{-9}T^5 \end{aligned}$$

The salinity is related to chloride concentration by (Thomann and Mueller 1987),

$$S = 1.80655 \times 10^{-3} Cl$$

where Cl = chloride concentration. The chloride concentration is related to conductivity by

$$\begin{array}{ll} Cl = 0 & \text{Cond} < 84.2 \mu\text{mhos} \\ Cl = 0.3091 \times \text{Cond} - 26.021 & \text{Cond} \geq 84.2 \mu\text{mhos} \end{array}$$

8 APPENDIX B: O'CONNOR'S GAS TRANSFER MODEL

O'Connor (1983) has developed a theoretically based set of formulas to compute gas transfer for low-solubility gases such as oxygen. Three different formulas are used depending on the wind speed,

Smooth surfaces ($U_w < 6$ m/s):

$$K_l = \left(\frac{D_{ox}}{\nu_w} \right)^{2/3} \sqrt{C_d \frac{\rho_a}{\rho_w} \frac{\kappa^{1/3}}{\Gamma_0}} U_w \quad (153)$$

where D_{ox} = the diffusivity of oxygen in water [cm s^{-2}], ν_w = the viscosity of water [cm s^{-2}], C_d = drag coefficient, ρ_a = air density [g cm^{-3}], ρ_w = water density [$= 1 \text{ g cm}^{-3}$], κ = the Von Karman constant ($= 0.4$), and Γ_0 = a Reynold's number. Several of the model parameters are related to air and water temperature as in

$$D_{ox} = 0.000000458T_1 + 0.000012 \quad (154)$$

$$\nu_w = 0.0164 - 0.00024514T_1 \quad (155)$$

$$\rho_a = 0.00129 - 0.000004T_{air} \quad (156)$$

Transitional surfaces ($6 \text{ m/s} \leq U_w \leq 20 \text{ m/s}$):

$$\frac{1}{K_l} = \frac{1}{\left(\frac{D_{ox}}{\nu_w} \right)^{2/3} \frac{\kappa^{1/3}}{\Gamma(U_*)} \sqrt{\frac{\rho_a}{\rho_w} U_*}} + \frac{1}{\sqrt{\frac{D_{ox} U_*}{\kappa z_0(U_*)} \frac{\rho_a \nu_a}{\rho_w \nu_w}}} \quad (157)$$

where ν_a = the viscosity of air [cm s^{-2}]. Other parameters are tabulated (Table 6) or calculated as

$$\nu_a = 0.133 + 0.0009T_{air} \quad (158)$$

$$\Gamma(U_*) = \Gamma_0 \frac{U_*}{U_{*c}} e^{-U_*/U_{*c} + 1} \quad (159)$$

$$z_0(U_*) = \frac{1}{1/z_e + \lambda_1 e^{-U_*/U_{*t}}} \quad (160)$$

$$U_* = \sqrt{C_d} U_w \quad (161)$$

Table 6 Parameters for O'Connor gas transfer model. Note that at present, Lake2K uses the large scale parameters.

Scale	λ_1	U_{*t}	Γ_0	U_{*c}	z_e
Small	10	9	10	22	0.25

Intermediate	3	10	6.5	11	0.25
Large	3	10	5	11	0.35

Rough surfaces ($U_w > 20$ m/s):

$$K_l = \sqrt{\frac{D_{ox}}{\kappa z_e} \frac{\rho_a v_a}{\rho_w v_w} \sqrt{C_d} U_w} \quad (162)$$

Note that the drag coefficient is required to implement the foregoing equations. The following formula relates the drag coefficient to wind speed and other characteristics of the air-water interface

$$\frac{1}{\sqrt{C_d}} = \frac{1}{\kappa} \ln \left[\frac{1000}{z_e} + \frac{1000 \lambda_1 \sqrt{C_d} U_w}{v_a} e^{-\sqrt{C_d} U_w / U_{*t}} \right] \quad (163)$$

This equation is solved for C_d with the Newton-Raphson method.

9 REFERENCES

- APHA, 1995. Standard methods for the examination of water and wastewater, 19th Edn. American Public Health Association, American Water Works Association and Water Environment Federation: Washington, D.C.
- Ashton, G.D. (1986). River and Lake Ice Engineering. Littleton, CO, Water Resources Publications.
- Baly, E.C.C. 1935. The Kinetics of Photosynthesis. *Proc. Royal Soc. London Ser. B*, 117:218-239.
- Banks, R. B. 1975. "Some Features of Wind Action on Shallow Lakes." *J. Environ Engr. Div. ASCE*. 101(E5): 813-827.
- Banks, R. B. and Herrera, F. F. 1977. "Effect of Wind and Rain on Surface Reaeration." *J. Environ Engr. Div. ASCE*. 103(E3): 489-504.
- Baker, K.S. and Frouin, R. 1987. Relation between photosynthetically available radiation and total insolation at the ocean surface under clear skies. *Limnol. Oceanogr.* 1370-1377.
- Bowie, G.L., Mills, W.B., Porcella, D.B., Campbell, C.L., Pagenkopf, J.R., Rupp, G.L., Johnson, K.M., Chan, P.W.H., Gherini, S.A. and Chamberlin, C.E. 1985. Rates, Constants, and Kinetic Formulations in Surface Water Quality Modeling. U.S. Envir. Prot. Agency, ORD, Athens, GA, ERL, EPA/600/3-85/040.
- Brady, D.K., Graves, W.L., and Geyer, J.C. 1969. Surface Heat Exchange at Power Plant Cooling Lakes, Cooling Water Discharge Project Report, No. 5, Edison Electric Inst. Pub. No. 69-901, New York, NY.
- Bras, R.L. 1990. Hydrology. Addison-Wesley, Reading, MA.
- Brunt, D. 1932. Notes on radiation in the atmosphere: I. *Quart J Royal Meteorol Soc* 58:389-420.
- Brutsaert, W. 1982. Evaporation into the atmosphere: theory, history, and applications. D.Reidel Publishing Co., Hingham MA, 299 p.
- Cerco, C.F. and Cole, T. 1994. Three-Dimensional Eutrophication Model of Chesapeake Bay. Vol. 1: Main Report. U.S. Army Corps of Engineers. Waterways Experiment Station Tech. Report EL-94-4.
- Chapra and Canale 2002. *Numerical Methods for Engineers*, 4th Ed. New York, McGraw-Hill.
- Chapra, S.C. 1997. *Surface water quality modeling*. New York, McGraw-Hill.
- Chapra, S.C.; Camacho, L.A.; McBride, G.B. 2021. Impact of Global Warming on Dissolved Oxygen and BOD Assimilative Capacity of the World's Rivers: Modeling Analysis. *Water*, 13, 2408. <https://doi.org/10.3390/w13172408>.
- Di Toro, D.M. 1978. Optics of Turbid Estuarine Waters: Approximations and Applications. *Water Res.* 12:1059-1068.
- Di Toro, D.M. 2001. *Sediment Flux Modeling*. Wiley-Interscience, New York, NY.
- Di Toro, D. M. and J. F. Fitzpatrick. 1993. Chesapeake Bay sediment flux model. Tech. Report EL-93-2, U.S. Army Corps of Engineers, Waterways Experiment Station, Vicksburg, Mississippi, 316 pp.
- Di Toro, D.M, Paquin, P.R., Subburamu, K. and Gruber, D.A. 1991. Sediment Oxygen Demand Model: Methane and Ammonia Oxidation. *J. Environ. Eng.*, 116(5):945-986.
- Edinger, J.E., Brady, D.K., and Geyer, J.C. 1974. Heat Exchange and Transport in the Environment. Report No. 14, EPRI Pub. No. EA-74-049-00-3, Electric Power Research Institute, Palo Alto, CA.
- Harbeck, G. E., 1962, A practical field technique for measuring reservoir evaporation utilizing mass-transfer theory. US Geological Survey Professional Paper 272-E, 101-5.
- Helfrich, K.R., E.E. Adams, A.L. Godbey, and D.R.F. Harleman. 1982. Evaluation of models for predicting evaporative water loss in cooling impoundments. Report CS-2325, Research project 1260-17. Electric Power Research Institute, Palo Alto, CA. March 1982.

- Henderson-Sellers, B. 1984. Engineering Limnology. Boston, MA, Pitman.
- Hutchinson, G.E. 1957. *A Treatise on Limnology, Vol. 1, Physics and Chemistry*. Wiley, New York, NY.
- Kirk, J.T.O. 1994. Light and Photosynthesis in Aquatic Systems. Cambridge, UK, Cambridge University Press.
- Koberg, G.E. 1964. Methods to compute long-wave radiation from the atmosphere and reflected solar radiation from a water surface. US Geological Survey Professional Paper 272-F.
- Laws, E. A. and Chalup, M. S. 1990. A Microalgal Growth Model. *Limnol. Oceanogr.* 35(3):597-608.
- LI-COR, 2003. Radiation Measurement Instruments, LI-COR, Lincoln, NE, 30 pp.
- Mackay, D. and Yeun, A.T.K. 1983. Mass Transfer Coefficient Correlations for Volatilization of Organic Solutes from Water. *Environ. Sci. Technol.* 17:211-233.
- Marciano, J.K. and G.E. Harbeck. 1952. Mass transfer studies in water loss investigation: Lake Hefner studies. Geological Circular 229. U.S. Geological Survey, Washington DC.
- Martin, J.L. and McCutcheon. 1999. Hydrodynamics and Transport for Water Quality Models. Boca Raton, FL, Lewis Publishers.
- Meeus, J. 1999. Astronomical algorithms. Second edition. Willmann-Bell, Inc. Richmond, VA.
- Millero, F. J. and Poisson, A. 1981. "International One-Atmosphere Equation of State for Sea Water." *Deep-Sea Res. (Part A)*. 28(6A):625-629.
- Munk, W.H. and Anderson, E.R. 1948. Notes on a Theory of the Thermocline. *J. Marine Res.* 6:76-84.
- O'Connor, D.J. 1983. Wind Effects on Gas-Liquid Transfer Coefficients. *Journal of Environmental Engineering*, 109(3):731-752.
- Preisendorfer, R.W. 1986. Secchi Disc Science: Visual Optics of Natural Waters. *Limnol. Oceanogr.* 31(5):909-926.
- Raudkivi, A. I. 1979. *Hydrology*. Pergamon, Oxford, England.
- Redfield, A.C., Ketchum, B.H. and Richards, F.A. 1963. The Influence of Organisms on the Composition of Seawater, in *The Sea*, M.N. Hill, ed. Vol. 2, pp. 27-46, Wiley-Interscience, NY.
- Riley, G.A. 1956. Oceanography of Long Island Sound 1952-1954. II. Physical Oceanography, *Bull. Bingham Oceanog. Collection* 15, pp. 15-16.
- Ryan, P.J. and D.R.F. Harleman. 1971. Prediction of the annual cycle of temperature changes in a stratified lake or reservoir. Mathematical model and user's manual. Ralph M. Parsons Laboratory Report No. 137. Massachusetts Institute of Technology. Cambridge, MA.
- Ryan, P.J. and K.D. Stolzenbach. 1972. Engineering aspects of heat disposal from power generation, (D.R.F. Harleman, ed.). R.M. Parson Laboratory for Water Resources and Hydrodynamics, Department of Civil Engineering, Massachusetts Institute of Technology, Cambridge, MA.
- Shanahan, P. 1984. Water temperature modeling: a practical guide. In: Proceedings of stormwater and water quality model users group meeting, April 12-13, 1984. USEPA, EPA-600/9-85-003. (users.rcn.com/shanahan.ma.ultranet/TempModeling.pdf)
- Smith, E.L. 1936. Photosynthesis in Relation to Light and Carbon Dioxide. *Proc. Natl. Acad. Sci.* 22:504-511.
- Steele, J.H. 1962. Environmental Control of Photosynthesis in the Sea. *Limnol. Oceanogr.* 7:137-150.
- Stumm, W. and Morgan, J.J. 1996. Aquatic Chemistry, New York, Wiley-Interscience, 1022 pp.
- Szeicz, G. 1974. Solar radiation for plant growth. *J. Appl. Ecol.* 11:617-636.
- Thomann, R.V. and Mueller, J.A. 1987. Principles of Surface Water Quality Modeling and Control. New York, Harper-Collins.
- Tyler, J.E. 1968. The Secchi Disc. *Limnol. Oceanogr.* 13(1):1-6.

- TVA, 1972. Heat and mass transfer between a water surface and the atmosphere. Water Resources Research, Laboratory Report No. 14. Engineering Laboratory, Division of Water Control Planning, Tennessee Valley Authority, Norris TN.
- Wanninkhof, R., Ledwell, I. R., and Crusius, I. 1991. "Gas Transfer Velocities on Lakes Measured with Sulfur Hexafluoride." In Symposium Volume of the Second International Conference on Gas Transfer at Water Surfaces, S.C. Wilhelms and I.S. Gulliver, eds., Minneapolis, MN .